Combined dynamics of magnetization and particle rotation of a suspended superparamagnetic particle in the presence of an orienting field: semi-analytical and numerical solution

OPEN ACCESS
Mathematical Models and Methods in Applied Sciences
Vol. 32, No. 7 (2022) 1349–1383

DOI: 10.1142/S0218202522500300

Combined dynamics of magnetization and particle rotation of a suspended superparamagnetic particle in the presence of an orienting field: Semi-analytical and numerical solution

Martin Kröger*
Polymer Physics, Department of Materials,
ETH Zurich, CH-8093 Zurich, Switzerland
mk@mat.ethz.ch

Patrick Ilg
School of Mathematical, Physical, and Computational Sciences,
University of Reading, Reading, RG6 6AX, UK
p.ilg@reading.ac.uk

Received 29 July 2021
Revised 14 March 2022
Accepted 8 April 2022
Published 21 June 2022
Communicated by Y. Bazilevs

The magnetization dynamics of suspended superparamagnetic particles is governed by internal Néel relaxation as well as Brownian diffusion of the whole particle. We here present semi-analytical and numerical solutions of the kinetic equation, describing the combined rotation of particle orientation and magnetization. The solutions are based on an expansion of the joint probability density into a complete set of bipolar harmonics, leading to a coupled set of ordinary differential equations for the expansion coefficients. Extending previous works, we discuss the spectrum of relaxation times as well as convergence and limits of applicability of the method. Furthermore, we also provide the numerical scheme in electronic form, so that readers can readily implement and use the model.

Keywords: Nanoparticles; magnetization; Fokker–Planck equation; Langevin dynamics; moment expansion; egg model; bipolar spherical harmonics.

AMS Subject Classification 2020: 82Cxx, 82D40, 82D80, 78M05, 82C31

*Corresponding author.

1. Introduction

Magnetic nanoparticles that are suspended in non-magnetic carrier fluids provide interesting model systems.[15] Several recent works deal with the simulation of suspended magnetic nanoparticles in fluid flow.[28,30] Their superparamagnetic behavior allows for promising applications that lead to renewed interest in their dynamic properties.[26] While considerable progress has been made in recent years for the limiting cases of immobile or thermally blocked particles,[3,11,14,15,26] the general case turns out to be more difficult to handle. This is especially true in the presence of external magnetic fields, which is not only theoretically interesting, but also highly relevant for several applications.[5,20]

Two basic relaxation mechanisms are present for suspended magnetic nanoparticles: internal Néel relaxation of the magnetization and Brownian rotational diffusion of the whole particle.[15] The so-called "egg" model of Shliomis and Stepanov[23,24] provides a physically sound, microscopic starting point to investigate nanoparticle dynamics including the combined effect of these two relaxation mechanisms. Some previous works used stochastic simulations to study this model.[2,5,7,21,22] However, stochastic simulations are often time-consuming due to the inherent noise. Alternative approaches by numerically solving the corresponding kinetic (Fokker–Planck) equation therefore bear some advantages. A previous work along these lines was limited to axis-symmetric solutions.[18]

Here, we follow more recent works[17] and expand the joint probability density in a complete basis set to solve the egg model also for general situations. We re-derive the coupled system of linear ordinary differential equations for the expansion coefficients in matrix form. Since the resulting expressions are rather cumbersome, we here provide them numerically in electronic form, which allows readers to straightforwardly implement the model. We validate the implementation by testing the numerical results versus analytical expressions for limiting cases and discuss convergence properties. Furthermore, we also compare our numerical results to stochastic simulations of the corresponding Langevin equations. We also provide the spectrum of relaxation times of the Fokker–Planck equation for several model parameters. Since the number of relevant terms in the expansion grows rapidly for strong magnetic fields, we also discuss limits of practical applicability of this method.

2. Microscopic Egg Model

In the microscopic "egg" model proposed by Shliomis and Stepanov,[23,24] the state of a magnetic nanoparticle is described by two three-dimensional unit vectors, $\mathbf{e}$ and $\mathbf{n}$, denoting the orientation of the particle's magnetic moment and easy axis, respectively (see Fig. 1). The potential energy of a magnetic nanoparticle in the presence of an external magnetic field $\mathbf{H}$ is given by the sum of the Zeeman energy and the anisotropy contribution

$$U(\mathbf{e},\mathbf{n}) = -m\mathbf{e}\cdot\mathbf{H} - Kv_{\mathrm{m}}(\mathbf{e}\cdot\mathbf{n})^2. \tag{2.1}$$

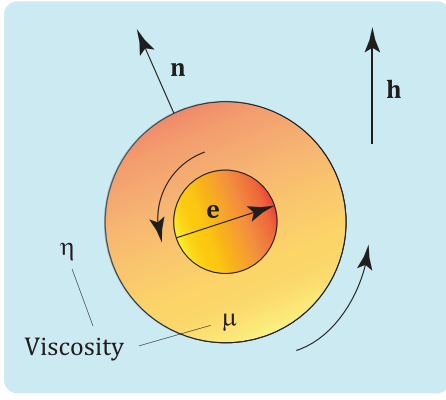

Fig. 1. (Color online) Schematic of the egg model: the magnetic core (yolk) with magnetization direction $\mathbf{e}$ is embedded in a non-magnetic background (white) with effective viscosity μ. The particle (egg) is oriented along the easy axis $\mathbf{n}$, suspended in a liquid with viscosity η, and subjected to an external magnetic field $\mathbf{h}$ aligned in z-direction.

The magnetic moment and the magnetic volume of the nanoparticle are denoted by m and v_{m}, respectively, and K denotes the anisotropy constant of the magnetic material. From the potential energy relative to thermal energy

$$\beta U(\mathbf{e},\mathbf{n}) = -\mathbf{e}\cdot\mathbf{h} - \kappa(\mathbf{e}\cdot\mathbf{n})^2 \tag{2.2}$$

with the inverse thermal energy $\beta = 1/k_{\mathrm{B}}T$, we define the dimensionless anisotropy constant $\kappa = \beta K v_{\mathrm{m}}$ and the dimensionless field $\mathbf{h} = \beta m\mathbf{H}$, with $h = |\mathbf{h}|$ the Langevin parameter.

The combined dynamics of magnetization and particle rotation in a viscous medium is described by the following Fokker–Planck (FP) equation[3,23] for the time-dependent joint probability density $F(\mathbf{e},\mathbf{n};t)$,

$$\frac{\partial F}{\partial t} = -\boldsymbol{\mathcal{L}}_e\cdot(\boldsymbol{\omega}_{\mathrm{L}}F) + \left(\frac{1}{2\tau_{\mathrm{B}}}\boldsymbol{\mathcal{L}}\cdot F\boldsymbol{\mathcal{L}} + \frac{1}{2\tau_{\mathrm{D}}}\boldsymbol{\mathcal{L}}_e\cdot F\boldsymbol{\mathcal{L}}_e\right)(\beta U + \ln F). \tag{2.3}$$

In Eq. (2.3), we defined the rotational operators $\boldsymbol{\mathcal{L}}_e = \mathbf{e}\times\partial/\partial\mathbf{e}$, $\boldsymbol{\mathcal{L}}_n = \mathbf{n}\times\partial/\partial\mathbf{n}$ and $\boldsymbol{\mathcal{L}} = \boldsymbol{\mathcal{L}}_e + \boldsymbol{\mathcal{L}}_n$. For fixed easy axis, Eq. (2.3) reduces to the Landau-Lifshitz-Gilbert magnetization equation,[4,5] whereas the rigid-dipole approximation of Brownian rotational dynamics is recovered by considering the dynamics of $\mathbf{n}$ only and identifying $\mathbf{e}$ and $\mathbf{n}$ in the internal energy U.

There are two basic time scales appearing in Eq. (2.3) that we already mentioned in the introduction: (i) the Brownian relaxation time of rotational diffusion of the particle in a liquid with viscosity η,

$$\tau_{\mathrm{B}} = 3\beta\eta v_{\mathrm{h}} \tag{2.4}$$

with v_{h} the hydrodynamic volume of the nanoparticles; (ii) the internal magnetization time

$$\tau_{\mathrm{D}} = \frac{\beta m}{2\alpha\gamma} \tag{2.5}$$

with the dimensionless damping parameter α and the gyromagnetic ratio γ. Formally, τ_{D} can also be written as $\tau_{\mathrm{D}} = 3\beta\mu v_m$, where μ denotes an effective viscosity. Finally, the Larmor frequency is defined by $\boldsymbol{\omega}_{\mathrm{L}} = -(\gamma/m)\partial U/\partial \mathbf{e}$ and is given here by $\boldsymbol{\omega}_{\mathrm{L}} = \gamma\mathbf{H} + 2KM_{\mathrm{s}}^{-1}(\mathbf{e}\cdot\mathbf{n})\mathbf{n}$, where M_{s} denotes the spontaneous magnetization of the magnetic material, $M_{\mathrm{s}} = m/v_{\mathrm{m}}$.

We note that a modified egg model has been studied in Refs. 29 and 25 where the operator $\boldsymbol{\mathcal{L}}$ in Eq. (2.3) is replaced by $\boldsymbol{\mathcal{L}}_n$. By construction, the stationary Boltzmann equilibrium solution $F^{\mathrm{stat}} \sim \exp(-\beta U)$ remains unaffected by this modification. Note that in the absence of a magnetic field and no anisotropy energy, the free relaxation is determined by τ_{D} in the modified model of Refs. 29 and 25, whereas it is the correct, effective relaxation time τ_0 defined by $\tau_0^{-1} = \tau_{\mathrm{D}}^{-1} + \tau_{\mathrm{B}}^{-1}$ for the original model of Shliomis and Stepanov.[23] Further physical arguments for the occurrence of the operator $\boldsymbol{\mathcal{L}}$ are convincingly presented in Ref. 23. Therefore, we stick to the original egg model in the following. In Appendix G we summarize the corresponding treatment of the model studied in Refs. 29 and 25.

3. Methods

We are going to consider any superposition of collinear static and oscillating external fields defining the z-axis

$$\mathbf{h}(t) = h(t)\mathbf{e}_z = \left(h_0 + h_1 e^{i\omega t}\right)\mathbf{e}_z \tag{3.1}$$

with the two time t-independent amplitudes h_0, h_1 and frequency ω.

3.1. *Moment expansion using bipolar spherical harmonics*

While every scalar function depending on a single, three-dimensional unit vector $\mathbf{e} = \mathbf{e}_x\cos\phi\sin\theta + \mathbf{e}_y\sin\phi\sin\theta + \mathbf{e}_z\cos\theta$ can conveniently be expanded into an orthonormal basis set of spherical harmonics by way of the associated Legendre polynomials P_l^m,

$$Y_{lm}(\mathbf{e}) = \sqrt{\frac{2l+1}{4\pi}}\sqrt{\frac{(l-m)!}{(l+m)!}}\,P_l^m(\mathbf{e}\cdot\mathbf{e}_z)e^{im\phi} \tag{3.2}$$

with integer-valued $l \geq 0$ and $|m| \leq l$, and the orthonormality feature $\int Y_{lm}^* Y_{l'm'}\,d\mathbf{e} = \delta_{ll'}\delta_{mm'}$, a function that depends on the two independent unit vectors $\mathbf{e}$ and $\mathbf{n}$ can analogously be expanded using bipolar spherical harmonics Y_K. Bipolar harmonics are bilinear products of spherical harmonics with different arguments coupled to total angular momentum L,

$$Y_K(\mathbf{e},\mathbf{n}) = \sum_{m_1=-l_1}^{l_1}\sum_{m_2=-l_2}^{l_2} C_{l_1 m_1 l_2 m_2}^{LM} Y_{l_1,m_1}(\mathbf{e})Y_{l_2,m_2}(\mathbf{n}), \tag{3.3}$$

where K stands for a multi-index

$$K = {}_{l_1 l_2}^{LM} \tag{3.4}$$

whose indices can take the following values: $l_1, l_2 \geq 0$, $|l_1 - l_2| \leq L \leq l_1 + l_2$ and $|M| \leq L$.[27] The numerical coefficients $C^{LM}_{l_1 m_1 l_2 m_2}$ occurring in (3.3) are the known Clebsch–Gordan coefficients (Appendix D) that are chosen to ensure orthonormality of the bipolar harmonics

$$\langle Y_K | Y_{K'} \rangle = \iint Y_K^*(\mathbf{e}, \mathbf{n}) Y_{K'}(\mathbf{e}, \mathbf{n}) \, d\mathbf{e} d\mathbf{n} = \delta_{K,K'}, \tag{3.5}$$

where each integral is taken over the three-dimensional unit sphere. For this reason $Y_{00}^{00} = (4\pi)^{-1}$. As for spherical harmonics, one has the freedom to choose the orientation of the coordinate system. For convenience, we have chosen in Eq. (3.1) to align the $\mathbf{e}_z$-axis of the coordinate system to coincide with the direction of the dimensionless external, eventually time-dependent magnetic field $\mathbf{h}(t)$.

Because bipolar harmonics constitute a complete set of basis functions, every function $X(\mathbf{e}, \mathbf{n})$ can be written as $X = \sum_K x_K Y_K$ with numerical coefficients x_K that can be calculated via $x_K = \langle Y_K | X \rangle$ thanks to (3.5). In practice, for an arbitrarily complex function, the infinite sum has to be approximated by a finite sum, and the remaining terms are neglected, in the absence of a suitable closure approximation.[12] We denote by Oth order bipolar expansion a summation over all such K whose largest absolute index is denoted by O. From the mentioned inequalities follows the number of such multi-indices. Up to order O one has

$$I(O) = \sum_{l_1=0}^{O} \sum_{l_2=0}^{O} \sum_{L=|l_1-l_2|}^{\min(O, l_1+l_2)} \sum_{M=-L}^{L} 1 = \left(1 + \frac{7}{6}O + \frac{7}{12}O^2\right)(1+O)^2 \tag{3.6}$$

different multi-indices K, including $K = {}^{00}_{00}$. The expression evaluates to $I(1) = 11$, $I(2) = 51$, $I(6) = 1421$, $I(8) = 3861$, $I(10) = 8591$ etc. and scales $\sim O^4$ for large O. For comparison, the number of spherical harmonics up to order O is $(1+O)^2$. Due to the inequalities $I(O) < (1+O)^4$, and only about $7/12 \approx 58\%$ of possible Y_{lm} combinations are present in Y_K, for large O.

For a beginning, let us express the unit vectors $\mathbf{e}$ and $\mathbf{n}$ in terms of bipolar harmonics

$$\mathbf{e} = \frac{4\pi}{\sqrt{3}} \begin{pmatrix} \frac{1}{\sqrt{2}}\left(Y_{10}^{1,-1} - Y_{10}^{1,1}\right) \\ \frac{i}{\sqrt{2}}\left(Y_{10}^{1,-1} + Y_{10}^{1,1}\right) \\ Y_{10}^{10} \end{pmatrix}, \quad \mathbf{n} = \frac{4\pi}{\sqrt{3}} \begin{pmatrix} \frac{1}{\sqrt{2}}\left(Y_{01}^{1,-1} - Y_{01}^{1,1}\right) \\ \frac{i}{\sqrt{2}}\left(Y_{01}^{1,-1} + Y_{01}^{1,1}\right) \\ Y_{01}^{10} \end{pmatrix}, \tag{3.7}$$

where we stripped the argument $(\mathbf{e}, \mathbf{n})$ from the bipolar harmonics, and where we used the classical vector notation with respect to the Euclidean basis $\mathbf{e}_x$, $\mathbf{e}_y$ and $\mathbf{e}_z$, so that Eq. (3.7) implies

$$\mathbf{e} \cdot \mathbf{h}(t) = h(t) \mathbf{e} \cdot \mathbf{e}_z = \frac{4\pi}{\sqrt{3}} h(t) Y_{10}^{10}, \tag{3.8}$$

$$(\mathbf{e} \cdot \mathbf{n})^2 - \frac{1}{3} = \frac{8\pi}{\sqrt{45}} Y_{22}^{00}. \tag{3.9}$$

Relationships between some other Y_K and the base vectors are mentioned in Appendix A. Recall that the right-hand sides of these expressions are the evaluated infinite sums $X = \sum_K \langle Y_K|X\rangle Y_K$, if X denotes the corresponding left-hand side. Up to here, bipolar harmonics of order $O = 2$ were sufficient to write down identities.

A more tedious but important exercise is the evaluation of brackets if X is the product of two bipolar harmonics, such as Y_K and Y_Q,

$$X = Y_K(\mathbf{e},\mathbf{n})Y_Q(\mathbf{e},\mathbf{n}) = \sum_{K'} \langle Y_{K'}|X\rangle Y_{K'}, \tag{3.10}$$

as all the integrands in the double integrals are products of six spherical harmonics. A summation $\sum_K$ such as the one occurring in Eq. (3.10) actually stands for a four-fold sum over the four indices hidden in K, to be specific

$$\sum_K \cdots = \sum_{l_1=0}^{\infty} \sum_{l_2=0}^{\infty} \sum_{L=|l_1-l_2|}^{l_1+l_2} \sum_{M=-L}^{L} \cdots. \tag{3.11}$$

The problem of explicitly calculating all non-vanishing matrix elements in Eq. (3.10) up to some order O had already been solved in the last millenium.[27] In short, one has to make use of Wigner $9j$-symbols, Wigner $6j$-symbols and Clebsch–Gordan coefficients, and to perform nested sums over these coefficients. Details of such straightforward calculations are collected in Appendix D. Fortunately, the only multi-indices Q required within the context of this study are $Q = \binom{10}{10}$ and $Q = \binom{00}{22}$, i.e. we are going to make use of

$$Y_K Y_{10}^{10} = \sum_{K'} \mathcal{P}_K^{K'} Y_{K'}, \tag{3.12}$$

$$Y_K Y_{22}^{00} = \sum_{K'} \mathcal{Q}_K^{K'} Y_{K'}, \tag{3.13}$$

where the numerical coefficients $\mathcal{P}_K^{K'} = \langle Y_{K'}|Y_K Y_{10}^{10}\rangle$ and similarly $\mathcal{Q}_K^{K'}$ can be considered known up to order O. They are explicitly given as yet unevaluated sums over Clebsch–Gordan and Wigner 9j-symbols by (D.5) and (D.6) of Appendix D. Each of them is a sparse square $I(O) \times I(O)$ matrix. For readers' convenience, we provide them up to $O = 10$ as part of our supplementary material. Some important symmetry properties of $\mathcal{P}$ and $\mathcal{Q}$ will be used later on,

$$\mathcal{P}_K^{K'} \propto \delta_{M,M'}\delta_{l_2,l_2'}, \tag{3.14}$$

$$\mathcal{Q}_K^{K'} \propto \delta_{M,M'}\delta_{L,L'}, \tag{3.15}$$

so that we may write more explicitly

$$Y_K Y_{10}^{10} = \sum_{l_1'=0}^{\infty} \sum_{L'=|l_1'-l_2'|}^{l_1'+l_2'} \mathcal{P}_K^{\substack{L'M \\ l_1'l_2}} Y_{l_1'l_2}^{L'M}, \tag{3.16}$$

$$Y_K Y_{22}^{00} = \sum_{l_1'=0}^{\infty} \sum_{l_2'=0}^{\infty} \mathcal{Q}_K^{l_1' l_2'^{LM}} Y_{l_1' l_2'}^{LM} \tag{3.17}$$

to highlight double instead of quartic sums.

We should note in passing that irreducible tensors constructed from $\mathbf{e}$ and $\mathbf{n}$, such as multiple-rank anisotropic tensors[6] could be used instead of bipolar harmonics to expand a scalar function $X(\mathbf{e}, \mathbf{n})$. Since there is a one-to-one, albeit nontrivial, correspondence between anisotropic tensors and spherical and thus also bipolar spherical harmonics, there is no *a-priori*-advantage of one of the two approaches. We choose to use bipolar harmonics in this work. In essence, for any given order O, the moment expansion approach will result in linear system of differential equations that can be solved by matrix inversion (better, Gaussian elimination), and the true solution $F(\mathbf{e}, \mathbf{n}, t)$ of the FP equation is then approximated by its expansion into time-dependent moments. The FP equation for the probability density $F(\mathbf{e}, \mathbf{n}, t)$ is equivalent with a Langevin equation for the stochastic variables $\mathbf{e}_t$ and $\mathbf{n}_t$.

3.2. *Brownian dynamics*

To make the paper self-contained, we here recapitulate the derivation of the Langevin equations (see e.g. Refs. 23, 16, 8 and 5). In order to write down the stochastic differential equations for the random variables $\mathbf{e}_t$ and $\mathbf{n}_t$ corresponding to the egg model described in Sec. 2, let us rewrite the FP equation (2.3) in a more standard form

$$\frac{\partial F}{\partial t} = -\boldsymbol{\mathcal{L}}_e \cdot [\boldsymbol{\Omega}_e F] - \boldsymbol{\mathcal{L}}_n \cdot [\boldsymbol{\Omega}_n F] + \frac{1}{2} \begin{pmatrix} \boldsymbol{\mathcal{L}}_e \\ \boldsymbol{\mathcal{L}}_n \end{pmatrix} \begin{pmatrix} \boldsymbol{\mathcal{L}}_e \\ \boldsymbol{\mathcal{L}}_n \end{pmatrix} : \mathbf{D} F \tag{3.18}$$

with effective angular velocities given by

$$\boldsymbol{\Omega}_n = \frac{1}{2\tau_{\mathrm{B}}} \mathbf{e} \times \mathbf{h}, \tag{3.19}$$

$$\boldsymbol{\Omega}_e = \boldsymbol{\omega}_{\mathrm{L}} + \frac{1}{2\tau_0} \mathbf{e} \times \mathbf{h} + \frac{\kappa}{\tau_{\mathrm{D}}} (\mathbf{e} \cdot \mathbf{n}) \mathbf{e} \times \mathbf{n} \tag{3.20}$$

and the effective relaxation time τ_0 defined by $1/\tau_0 = 1/\tau_{\mathrm{D}} + 1/\tau_{\mathrm{B}}$. The diffusion matrix $\mathbf{D}$ is given by

$$\mathbf{D} = \begin{pmatrix} \tau_0^{-1} \mathbf{I} & \tau_{\mathrm{B}}^{-1} \mathbf{I} \\ \tau_{\mathrm{B}}^{-1} \mathbf{I} & \tau_{\mathrm{B}}^{-1} \mathbf{I} \end{pmatrix}, \tag{3.21}$$

where $\mathbf{I}$ denotes the three-dimensional unit matrix. We can decompose the diffusion matrix as $\mathbf{D} = \mathbf{B} \cdot \mathbf{B}^T$ with

$$\mathbf{B} = \begin{pmatrix} \tau_0^{-1/2} \mathbf{I} & \tau_{\mathrm{B}}^{-1/2} \mathbf{I} \\ \mathbf{0} & \tau_{\mathrm{B}}^{-1/2} \mathbf{I} \end{pmatrix}. \tag{3.22}$$

Finally noting that $\boldsymbol{\mathcal{L}}_e \cdot [\boldsymbol{\Omega}_e F] = \frac{\partial}{\partial \mathbf{e}} \cdot [\boldsymbol{\Omega}_e \times \mathbf{e} F]$, Eq. (3.18) is now in the standard form, so that we can read off the corresponding stochastic differential equations as[5,8,16]

$$\begin{pmatrix} d\mathbf{e}_t \\ d\mathbf{n}_t \end{pmatrix} = \begin{pmatrix} \boldsymbol{\Omega}_e \times \mathbf{e}_t \\ \boldsymbol{\Omega}_n \times \mathbf{n}_t \end{pmatrix} dt + \begin{pmatrix} \left[d\mathbf{W}_t^{(e)}/\sqrt{\tau_\mathrm{D}} + d\mathbf{W}_t^{(n)}/\sqrt{\tau_\mathrm{B}} \right] \times \mathbf{e}_t \\ d\mathbf{W}_t^{(n)}/\sqrt{\tau_\mathrm{B}} \times \mathbf{n}_t \end{pmatrix}. \tag{3.23}$$

These equations for $\mathbf{n}_t$, $\mathbf{e}_t$ agree with Eq. (15) in Ref. 23, where $\boldsymbol{\Omega}_e = \boldsymbol{\Omega}_n + \boldsymbol{\omega}_\mathrm{L} - (2\tau_\mathrm{D})^{-1} \boldsymbol{\mathcal{L}}_e(\beta U)$ is used. For later convenience, let us write this as $\boldsymbol{\Omega}_e = \boldsymbol{\Omega}_n + \boldsymbol{\omega}_e$ with

$$\boldsymbol{\omega}_e = \boldsymbol{\omega}_\mathrm{L} + \frac{1}{2\tau_\mathrm{D}} [\mathbf{e} \times \mathbf{h} + 2\kappa (\mathbf{e} \cdot \mathbf{n}) \mathbf{e} \times \mathbf{n}]. \tag{3.24}$$

Note the coupled noise in the magnetization dynamics which is modeled by independent, three-dimensional Wiener processes $\mathbf{W}_t^{(e)}$ and $\mathbf{W}_t^{(n)}$. We note that Shliomis and Stepanov derive Eq. (2.3) in Ref. 23 starting from the stochastic differential equations (3.23).

We integrate the stochastic differential equations (3.23) numerically using a weak second-order Heun algorithm with (i) predictor and (ii) corrector steps. (i) In the Heun predictor step, we calculate $\mathbf{n}^\mathrm{P} = \mathbf{n}'/|\mathbf{n}'|$ and $\mathbf{e}^\mathrm{P} = \mathbf{e}'/|\mathbf{e}'|$ with

$$\mathbf{n}' = \mathbf{n}_t + \Delta\boldsymbol{\omega}_t^{(n)} \times \mathbf{n}_t, \tag{3.25}$$

$$\mathbf{e}' = \mathbf{e}_t + \Delta\boldsymbol{\omega}_t^{(e)} \times \mathbf{e}_t, \tag{3.26}$$

where the angular velocity changes are calculated as

$$\Delta\boldsymbol{\omega}_t^{(n)} = \boldsymbol{\Omega}_n(t)\Delta t + \Delta\mathbf{W}_t^{(n)}, \tag{3.27}$$

$$\begin{aligned} \Delta\boldsymbol{\omega}_t^{(e)} &= \boldsymbol{\Omega}_e(t)\Delta t + \Delta\mathbf{W}_t^{(e)} + \Delta\mathbf{W}_t^{(n)} \\ &= \Delta\boldsymbol{\omega}_t^{(n)} + \boldsymbol{\omega}_e(t)\Delta t + \Delta\mathbf{W}_t^{(e)}, \end{aligned} \tag{3.28}$$

where Δt is the time step of integration, and $\Delta\mathbf{W}_t^{(n)}$, $\Delta\mathbf{W}_t^{(e)}$ the corresponding increments of three-dimensional, independent Gaussian processes with mean zero and variance $1/\tau_\mathrm{B}$ and $1/\tau_\mathrm{D}$, respectively. The vectors $\boldsymbol{\Omega}_n(t)$, $\boldsymbol{\Omega}_e(t)$ are obtained from Eqs. (3.19) and (3.20) upon inserting the current values of $\mathbf{n}_t$, $\mathbf{e}_t$. This predictor step corresponds to a first-order Euler–Maruyama scheme with additional normalization to ensure the predicted values $\mathbf{n}^\mathrm{P}$, $\mathbf{e}^\mathrm{P}$ are three-dimensional unit vectors.[16] (ii) In the second step of the Heun algorithm, we use these predicted values to calculate updated angular velocity increments $\Delta\bar{\boldsymbol{\omega}}^{(n)}$, $\Delta\bar{\boldsymbol{\omega}}^{(e)}$, which are obtained from Eqs. (3.27) and (3.28) when using $\mathbf{n}^\mathrm{P}$, $\mathbf{e}^\mathrm{P}$ instead of $\mathbf{n}_t$, $\mathbf{e}_t$ to evaluate $\boldsymbol{\Omega}_n$, $\boldsymbol{\Omega}_e$ from Eqs. (3.19) and (3.20).

Finally, the updated orientations at time $t + \Delta t$ are obtained from combining the predicted and corrected steps as

$$\mathbf{n}_{t+\Delta t} = \frac{\mathbf{n}_t + (1/2)\left[\Delta\boldsymbol{\omega}_t^{(n)} \times \mathbf{n}_t + \Delta\bar{\boldsymbol{\omega}}_t^{(n)} \times \mathbf{n}^\mathrm{P}\right]}{\left|\mathbf{n}_t + (1/2)\left[\Delta\boldsymbol{\omega}_t^{(n)} \times \mathbf{n}_t + \Delta\bar{\boldsymbol{\omega}}_t^{(n)} \times \mathbf{n}^\mathrm{P}\right]\right|}, \tag{3.29}$$

$$\mathbf{e}_{t+\Delta t} = \frac{\mathbf{e}_t + (1/2)\big[\Delta\boldsymbol{\omega}_t^{(e)} \times \mathbf{e}_t + \Delta\bar{\boldsymbol{\omega}}_t^{(e)} \times \mathbf{e}^{\mathrm{P}}\big]}{\big|\mathbf{e}_t + (1/2)\big[\Delta\boldsymbol{\omega}_t^{(e)} \times \mathbf{e}_t + \Delta\bar{\boldsymbol{\omega}}_t^{(e)} \times \mathbf{e}^{\mathrm{P}}\big]\big|}. \tag{3.30}$$

4. Results

We begin by expressing the energy U in terms of bipolar harmonics. With the help of Eqs. (3.1), (3.8) and (3.9) it can be written as[17]

$$\begin{aligned}\beta U &= -h(t)\mathbf{e}\cdot\mathbf{e}_z - \kappa(\mathbf{e}\cdot\mathbf{n})^2 \\ &= u_h Y_{10}^{10} + u_\kappa Y_{22}^{00} + \text{const.}\end{aligned} \tag{4.1}$$

with $\beta = 1/k_{\mathrm{B}}T$, and with the convenient abbreviations

$$u_h = -\frac{4\pi}{\sqrt{3}}h(t), \quad u_\kappa = -\frac{8\pi}{\sqrt{45}}\kappa. \tag{4.2}$$

Next, we expand the general joint probability density $F(\mathbf{e},\mathbf{n},t)$ solving the FP equation (2.3) in terms of bipolar spherical harmonics

$$F(\mathbf{e},\mathbf{n},t) = \frac{1}{4\pi}\sum_K b_K(t) Y_K(\mathbf{e},\mathbf{n}) \tag{4.3}$$

to find coupled equations of change for its time-dependent moments $b_K(t) = b_{l_1 l_2}^{LM}(t)$. The sum over the multi-index K is done as in Eq. (3.11). Because the FP equation is linear in F, it is sufficient to find the equation of change of Y_K, the time-evolution of the moments is then given by

$$\dot{b}_K = \sum_{K'} \langle Y_K | \dot{Y}_{K'} \rangle b_{K'}, \tag{4.4}$$

where the dot denotes a derivative with respect to time t. According to Eq. (2.3) the equation of change for Y_K reads

$$\dot{Y}_K = \left(\frac{1}{2\tau_{\mathrm{B}}}\boldsymbol{\mathcal{L}}\cdot Y_K\boldsymbol{\mathcal{L}} + \frac{1}{2\tau_{\mathrm{D}}}\boldsymbol{\mathcal{L}}_e\cdot Y_K\boldsymbol{\mathcal{L}}_e\right)(\beta U + \ln Y_K), \tag{4.5}$$

where we follow common practice and neglect the Larmor precession term, which is irrelevant below the GHz regime.[17] With the help of the basic identities

$$\begin{aligned}\boldsymbol{\mathcal{L}}(Y_K\boldsymbol{\mathcal{L}}U) &= (\boldsymbol{\mathcal{L}}Y_K)(\boldsymbol{\mathcal{L}}U) + Y_K\boldsymbol{\mathcal{L}}^2U, \\ \boldsymbol{\mathcal{L}}^2(Y_KU) &= 2(\boldsymbol{\mathcal{L}}U)(\boldsymbol{\mathcal{L}}Y_K) + U\boldsymbol{\mathcal{L}}^2Y_K + Y_K\boldsymbol{\mathcal{L}}^2U\end{aligned} \tag{4.6}$$

and exactly the same equations if $\boldsymbol{\mathcal{L}}$ is replaced by $\boldsymbol{\mathcal{L}}_e$. Equation (4.5) can be identically rewritten as (see also Ref. 17)

$$\begin{aligned}\dot{Y}_K = {}& \frac{1}{4\tau_B}\big[\boldsymbol{\mathcal{L}}^2(Y_K\beta U) + Y_K\boldsymbol{\mathcal{L}}^2(\beta U) + (2-\beta U)\boldsymbol{\mathcal{L}}^2Y_K\big] \\ & + \frac{1}{4\tau_D}\big[\boldsymbol{\mathcal{L}}_e^2(Y_K\beta U) + Y_K\boldsymbol{\mathcal{L}}_e^2(\beta U) + (2-\beta U)\boldsymbol{\mathcal{L}}_e^2Y_K\big].\end{aligned} \tag{4.7}$$

This version renders more convenient because we are left with squared operators $\boldsymbol{\mathcal{L}}^2$ and $\boldsymbol{\mathcal{L}}_e^2$ only, and because the Y_K are simultaneous eigenfunctions of these operators

$$\begin{aligned}\boldsymbol{\mathcal{L}}_e^2 Y_K &= -l_1(l_1+1)Y_K,\\ \boldsymbol{\mathcal{L}}_n^2 Y_K &= -l_2(l_2+1)Y_K,\\ \boldsymbol{\mathcal{L}}^2 Y_K &= -L(L+1)Y_K.\end{aligned} \tag{4.8}$$

The validity of these relationships and the eigenvalues follow from the corresponding property of the spherical harmonics, $\boldsymbol{\mathcal{L}}_e^2 Y_{lm}(\mathbf{e}) = -l(l+1)Y_{lm}(\mathbf{e})$ in concert with Eq. (3.3). Equation (4.8) with (4.1) furthermore imply

$$\begin{aligned}\boldsymbol{\mathcal{L}}_e^2(\beta U) &= -2u_h Y_{10}^{10} - 6u_\kappa Y_{22}^{00},\\ \boldsymbol{\mathcal{L}}^2(\beta U) &= -2u_h Y_{10}^{10}.\end{aligned} \tag{4.9}$$

The remaining terms in Eq. (4.7) of the form $\boldsymbol{\mathcal{L}}^2(Y_K \beta U)$ can be evaluated with the help of the constant matrices $\mathcal{P}$ and $\mathcal{Q}$ defined by Eqs. (3.12) and (3.13) as follows:

$$\begin{aligned}\boldsymbol{\mathcal{L}}^2(Y_K\beta U) &= u_h \boldsymbol{\mathcal{L}}^2\big(Y_K Y_{10}^{10}\big) + u_\kappa \boldsymbol{\mathcal{L}}^2\big(Y_K Y_{22}^{00}\big)\\ &= \sum_{K'} u_h \mathcal{P}_K^{K'} \boldsymbol{\mathcal{L}}^2(Y_{K'}) + u_\kappa \mathcal{Q}_K^{K'} \boldsymbol{\mathcal{L}}^2(Y_{K'})\\ &= -\sum_{K'} L'(L'+1)\big[u_h \mathcal{P}_K^{K'} + u_\kappa \mathcal{Q}_K^{K'}\big] Y_{K'}\end{aligned} \tag{4.10}$$

and

$$\begin{aligned}\boldsymbol{\mathcal{L}}_e^2(Y_K\beta U) &= u_h \boldsymbol{\mathcal{L}}_e^2\big(Y_K Y_{10}^{10}\big) + u_\kappa \boldsymbol{\mathcal{L}}_e^2\big(Y_K Y_{22}^{00}\big)\\ &= \sum_{K'} u_h \mathcal{P}_K^{K'} \boldsymbol{\mathcal{L}}_e^2 Y_{K'} + u_\kappa \mathcal{Q}_K^{K'} \boldsymbol{\mathcal{L}}_e^2 Y_{K'}\\ &= -\sum_{K'} l_1'\big(l_1'+1\big)\big[u_h \mathcal{P}_K^{K'} + u_\kappa \mathcal{Q}_K^{K'}\big] Y_{K'},\end{aligned} \tag{4.11}$$

where we made use of Eqs. (4.1) and (4.8). Finally inserting Eqs. (4.7)–(4.11) into Eq. (4.4), we end up with

$$\begin{aligned}\dot{b}_K = &-\frac{1}{\tau_K} b_K\\ &+ \frac{u_h}{4\tau_{\mathrm{B}}} \sum_{K'} b_{K'}[L'(L'+1) - L(L+1) - 2]\mathcal{P}_K^{K'}\\ &+ \frac{u_h}{4\tau_{\mathrm{D}}} \sum_{K'} b_{K'}[l_1'(l_1'+1) - l_1(l_1+1) - 2]\mathcal{P}_K^{K'}\\ &+ \frac{u_\kappa}{4\tau_{\mathrm{D}}} \sum_{K'} b_{K'}[l_1'(l_1'+1) - l_1(l_1+1) - 6]\mathcal{Q}_K^{K'},\end{aligned} \tag{4.12}$$

where one identifies the relaxation times τ_K relevant for the field- and interaction-free situation,

$$\tau_K = \left[\frac{L(L+1)}{2\tau_\mathrm{B}} + \frac{l_1(l_1+1)}{2\tau_\mathrm{D}}\right]^{-1}. \tag{4.13}$$

There is one term involving $\mathcal{Q}$ and proportional to u_κ that is apparently missing from Eq. (4.12). This term vanishes because of the property (3.15),

$$[L'(L'+1) - L(L+1)]\mathcal{Q}_K^{K'} \propto [L'(L'+1) - L(L+1)]\delta_{L,L'} = 0. \tag{4.14}$$

Note that Eq. (4.12) corrects a typo in Eq. (65) of Ref. 17.

Equation (4.12) is a coupled linear system of differential equations for the moments b_K. There is just one moment b_{00}^{00} which does not change in time as it represents the time-invariant normalization of F. The normalization $\iint F(\mathbf{e},\mathbf{n},t)\,d\mathbf{e}d\mathbf{n} = 1$ enforces $b_{00}^{00} = 1$ because of $Y_{00}^{00} = 1/4\pi$ and Eq. (4.3).

To simplify the notation and to allow for an efficient numerical implementation, we now collect all moments b_K with the exception of b_{00}^{00} into a vector $\mathbf{b}$. This vector has $I(n) - 1$ components, according to Eq. (3.6). Using vector notation, Eq. (4.12) can now be written as

$$\dot{\mathbf{b}} = -\mathbf{A}\cdot\mathbf{b} + \mathbf{d}, \tag{4.15}$$

where both, the square matrix $\mathbf{A}$ and vector $\mathbf{d}$ are determined by Eq. (4.12); the vector $\mathbf{d}$ arises from the terms where b_{00}^{00} was replaced by unity. It turns out that $\mathbf{d}$ has only two non-vanishing components, $^{10}_{10}$ and $^{00}_{22}$. Thus, component d_K of vector $\mathbf{d}$ is given by

$$d_K = \frac{h}{\sqrt{3}\tau_0}\delta_{K,{}^{10}_{10}} + \frac{2\kappa}{\sqrt{5}\tau_\mathrm{D}}\delta_{K,{}^{00}_{22}}. \tag{4.16}$$

As we prefer to collect all purely numerical factors in constant matrices $\mathbf{C}$ we write

$$\mathbf{A} = \frac{u_h}{\tau_\mathrm{B}}\mathbf{C}_\mathrm{Bh} + \frac{u_h}{\tau_\mathrm{D}}\mathbf{C}_\mathrm{Dh} + \frac{u_\kappa}{\tau_\mathrm{D}}\mathbf{C}_{\mathrm{D}\kappa} + \boldsymbol{\tau}^{-1}, \tag{4.17}$$

where $\boldsymbol{\tau}$ is a diagonal matrix with diagonal components given by τ_K, cf. Eq. (4.13). All the three constant matrices $\mathbf{C}_\mathrm{Bh}$, $\mathbf{C}_\mathrm{Dh}$ and $\mathbf{C}_{\mathrm{D}\kappa}$ have to be calculated once and for all using Eq. (4.12) and can in principle be stored for any given O. We provide all matrices for up to $O = 10$ as part of our supplementary data (Appendix H). Varying the model parameters τ_B, τ_D, $h(t)$ and κ then amounts to constructing $\mathbf{A}$ from Eqs. (4.13) and (4.17) without any effort (Appendix H).

Let us finish this paragraph with the equations of change for two selected moments,

$$b_{10}^{10} = \sqrt{3}\,\langle \mathbf{e}\cdot\mathbf{e}_z\rangle, \tag{4.18}$$

$$b_{22}^{00} = \frac{\sqrt{45}}{2}\left[(\mathbf{e}\cdot\mathbf{n})^2 - \frac{1}{3}\right], \tag{4.19}$$

according to Eq. (3.9). Their equations of change are given by the respective components of Eq. (4.15), where $\mathbf{A}\cdot\mathbf{b}$ and $\mathbf{d}$ given by Eqs. (4.16) and (4.17) evaluate to

$$\begin{aligned}
\frac{u_h}{\tau_\mathrm{B}}(\mathbf{C}_\mathrm{Bh}\cdot\mathbf{b})_{10}^{10} &= \frac{1}{\sqrt{15}}b_{20}^{20}\frac{h}{\tau_\mathrm{B}},\\
\frac{u_h}{\tau_\mathrm{D}}(\mathbf{C}_\mathrm{Dh}\cdot\mathbf{b})_{10}^{10} &= \frac{1}{\sqrt{15}}b_{20}^{20}\frac{h}{\tau_\mathrm{D}},\\
\frac{u_\kappa}{\tau_\mathrm{D}}(\mathbf{C}_{\mathrm{D}\kappa}\cdot\mathbf{b})_{10}^{10} &= \frac{2}{5\sqrt{3}}\left(\sqrt{\frac{3}{2}}b_{12}^{10}+b_{32}^{10}\right)\frac{\kappa}{\tau_\mathrm{D}},\\
(\boldsymbol{\tau}^{-1}\cdot\mathbf{b})_{10}^{10} &= b_{10}^{10}\tau_0^{-1},\\
d_{10}^{10} &= \frac{h}{\sqrt{3}\,\tau_0}
\end{aligned}\tag{4.20}$$

and

$$\begin{aligned}
\frac{u_h}{\tau_\mathrm{B}}(\mathbf{C}_\mathrm{Bh}\cdot\mathbf{b})_{22}^{00} &= 0,\\
\frac{u_h}{\tau_\mathrm{D}}(\mathbf{C}_\mathrm{Dh}\cdot\mathbf{b})_{22}^{00} &= \frac{1}{\sqrt{5}}\left(\sqrt{\frac{3}{2}}b_{12}^{10}+b_{32}^{10}\right)\frac{h}{\tau_\mathrm{D}},\\
\frac{u_\kappa}{\tau_\mathrm{D}}(\mathbf{C}_{\mathrm{D}\kappa}\cdot\mathbf{b})_{22}^{00} &= -\frac{2}{7}\left(b_{22}^{00}-\frac{4}{\sqrt{5}}b_{44}^{00}\right)\frac{\kappa}{\tau_\mathrm{D}},\\
(\boldsymbol{\tau}^{-1}\cdot\mathbf{b})_{22}^{00} &= 3b_{22}^{00}\tau_\mathrm{D}^{-1},\\
d_{22}^{00} &= \frac{2\kappa}{\sqrt{5}\,\tau_\mathrm{D}}.
\end{aligned}\tag{4.21}$$

The equations of change are coupled by the term involving b_{12}^{10} and b_{32}^{10} that appears in both equations. As we will see below, this term vanishes in the stationary regime.

4.1. *How do the moments couple?*

Bipolar harmonics are eigenfunctions of the Fokker–Planck operator for $h=\kappa=0$, Eq. (4.5). Therefore, the time evolution equations for the moments $\mathbf{b}$, Eq. (4.15), decouple in this case. In general, however, the moments couple directly to other moments by h and κ,

$$b_{l_1l_2}^{LM} \overset{h\neq 0}{\longleftrightarrow} b_{l_1\pm\{0,1\},l_2}^{L\pm\{0,1\},M},\tag{4.22}$$

$$b_{l_1l_2}^{LM} \overset{\kappa\neq 0}{\longleftrightarrow} b_{l_1\pm\{0,2\},l_2\pm\{0,2\}}^{L,M}.\tag{4.23}$$

This means that moments can potentially couple to up to at most 18 other moments when $h\neq 0$ and $\kappa\neq 0$. Usually there are less couplings because of the inequality $|l_1-l_2|\leq L\leq l_1+l_2$. For example, if $\kappa=0$, the moment b_{20}^{20} with $l_2=0$ can

just couple to the two moments b_{10}^{10} and b_{30}^{30} because of Eq. (4.22) and because the inequality implies $L = l_1$. If $h = 0$, the moment b_{44}^{00} with $L = 0$ can just couple to the two moments b_{22}^{00} and b_{66}^{00} because of Eq. (4.23) and because the inequality implies $l_1 = l_2$.

More importantly, even if $h \neq 0$ and $\kappa \neq 0$, there are sets of mutually independent moments. In particular, moments with even and odd l_2 are uncoupled, and those with different M are uncoupled as well. If the system is initially in an isotropic state, characterized by $b_{00}^{00} = 1$, moments with non-vanishing M or odd l_2 must remain at zero at all times, because the only non-vanishing components of the inhomogeneity $\mathbf{d}$, namely d_{10}^{10} and d_{22}^{00} have $M = 0$ and even $l_2 = 0$. Such moments include $\langle \mathbf{n} \cdot \mathbf{e} \rangle$ and $\langle \mathbf{n} \cdot \mathbf{e}_z \rangle$ according to Appendix A.

4.2. *Stationary moments of the probability density for time-independent h*

According to Eq. (4.15), stationary moments $\mathbf{b}_{\text{stat}}$ can be obtained upon inverting $\mathbf{A}$, using $\mathbf{b}^{\text{stat}} = \mathbf{A}^{-1} \cdot \mathbf{d}$. On the other hand, we know the stationary probability density exactly,

$$F^{\text{stat}}(\mathbf{e}, \mathbf{n}) = \frac{1}{Z} e^{-\beta U} = \frac{1}{Z} e^{-u_h Y_{10}^{10} - u_\kappa Y_{22}^{00}} = \frac{1}{4\pi} \sum_K b_K^{\text{stat}} Y_K \tag{4.24}$$

with normalization constant $Z = \int e^{-\beta U} \, d\mathbf{e} d\mathbf{n}$. Because of the form of the energy there are two types of ℓth moments that can be calculated analytically for any choice of model parameters: (i) $\left(b_{\ell 0}^{\ell 0}\right)_{\text{stat}}$ and (ii) $\left(b_{\ell\ell}^{00}\right)_{\text{stat}}$. We begin with case (i). Because $Y_{\ell 0}^{\ell 0}$ does not depend on $\mathbf{n}$, the integration over $\mathbf{n}$ simply contributes a factor 4π, and one obtains

$$\begin{aligned}
\left(b_{\ell 0}^{\ell 0}\right)_{\text{stat}} &= \int Y_{\ell 0}^{\ell 0} F^{\text{stat}} \, d\mathbf{e} d\mathbf{n} \\
&= \frac{4\pi \int Y_{\ell 0}^{\ell 0} e^{-u_h Y_{10}^{10}} \, d\mathbf{e}}{\int e^{-u_h Y_{10}^{10}} \, d\mathbf{e}} \\
&= \sqrt{2\ell + 1} \frac{\int P_\ell(\mathbf{e} \cdot \mathbf{e}_z) e^{h \mathbf{e} \cdot \mathbf{e}_z} \, d\mathbf{e}}{\int e^{h \mathbf{e} \cdot \mathbf{e}_z} \, d\mathbf{e}} \\
&= \sqrt{2\ell + 1} \frac{\int_{-1}^{1} P_\ell(z) e^{hz} \, dz}{\int_{-1}^{1} e^{hz} \, dz} = \sqrt{2\ell + 1} \, S_\ell, \\
S_\ell &= \langle P_\ell(\mathbf{e} \cdot \mathbf{e}_z) \rangle_{\text{stat}},
\end{aligned} \tag{4.25}$$

where the stationary order parameter S_ℓ is given by

$$S_\ell(h) = I_{\ell+1/2}(h) / I_{1/2}(h) \tag{4.26}$$

and where I is a modified spherical Bessel function of the first kind.[10] The order parameters obey the recursion relatation (see Appendix C)

$$S_{\ell+1}(h) = S_{\ell-1}(h) - (2\ell+1)h^{-1}S_\ell(h) \tag{4.27}$$

with $S_0(h) = 1$ and the Langevin function

$$S_1(h) = \mathcal{L}(h) = \coth(h) - h^{-1}. \tag{4.28}$$

For $\ell = 1, 2$, we obtain explicitly

$$\begin{aligned} \left(b_{10}^{10}\right)_{\text{stat}} &= \sqrt{3}\,\mathcal{L}(h), \\ \left(b_{20}^{20}\right)_{\text{stat}} &= \sqrt{5}\left(1 - \frac{3\mathcal{L}(h)}{h}\right). \end{aligned} \tag{4.29}$$

At small $h \ll 1$ (see also Eq. (4.37))

$$\left(b_{\ell 0}^{\ell 0}\right)_{\text{stat}} = a_\ell h^\ell + \mathcal{O}(h^{\ell+1}) \tag{4.30}$$

with coefficients (Appendix B)

$$a_\ell = \frac{\sqrt{\pi(2\ell+1)}}{2\Gamma(\ell+3/2)}. \tag{4.31}$$

For the special case of fully decoupled $\mathbf{e}$ and $\mathbf{n}$, i.e. $\kappa = 0$, the $\left(b_{\ell 0}^{\ell 0}\right)_{\text{stat}}$ are the only non-vanishing stationary moments.

Next, we treat case (ii). Because $Y_{\ell\ell}^{00}$ does only depend on the angle between $\mathbf{e}$ and $\mathbf{n}$, one obtains for any h and κ

$$\left(b_{\ell\ell}^{00}\right)_{\text{stat}} = \sqrt{2\ell+1}\frac{\displaystyle\int_{-1}^{1} P_\ell(z)e^{\kappa z^2}\,dz}{\displaystyle\int_{-1}^{1} e^{\kappa z^2}\,dz} = \sqrt{2\ell+1}\,\mathcal{S}_\ell,$$

$$\mathcal{S}_\ell = \langle P_\ell(\mathbf{e}\cdot\mathbf{n})\rangle_{\text{stat}}, \tag{4.32}$$

where we have introduced another order parameter $\mathcal{S}_\ell$ to be distinguished from S_ℓ defined by (4.25). The odd moments $\left(b_{\ell\ell}^{00}\right)_{\text{stat}}$ therefore vanish as $P_\ell(z)$ is antisymmetric in z for odd ℓ. The even moments can be calculated recursively via (see Appendix C)

$$\mathcal{S}_\ell = \frac{(2\ell-1)}{2\kappa\ell}\left[\frac{\sqrt{\kappa}}{2\text{Da}(\sqrt{\kappa})} - \sum_{k=1}^{\ell/2}(4k-3)\mathcal{S}_{2(k-1)}\right] - \frac{(\ell-1)\mathcal{S}_{\ell-2}}{\ell} \tag{4.33}$$

with $\mathcal{S}_0 = 1$ and where $\text{Da}(x) = e^{-x^2}\int_0^x e^{y^2}dy$ denotes the Dawson integral. The $\mathcal{S}_\ell$ can also be rewritten in terms of $\mathcal{S}_{\ell-2}$ and $\mathcal{S}_{\ell-4}$ alone (Appendix C),

$$\mathcal{S}_{\ell+2} = \frac{(2\ell+1)[3+2\kappa-4\ell(\ell+1)]}{2\kappa(\ell+2)(2\ell-1)}\mathcal{S}_\ell + \frac{(2\ell+3)(\ell-1)}{(\ell+2)(2\ell-1)}\mathcal{S}_{\ell-2}, \tag{4.34}$$

which requires $\mathcal{S}_2$ as input if used as recursion relation while Eq. (4.33) is more general. The first moments read

$$\begin{aligned}\left(b_{22}^{00}\right)_{\text{stat}} &= \sqrt{5}\left[\frac{3}{4\sqrt{\kappa}\text{Da}(\sqrt{\kappa})} - \frac{3}{4\kappa} - \frac{1}{2}\right],\\ \left(b_{44}^{00}\right)_{\text{stat}} &= 3\left[\frac{5(2\kappa-21)}{32\kappa^{3/2}\text{Da}(\sqrt{\kappa})} + \frac{3(\kappa+5)}{8\kappa} + \frac{105}{32\kappa^2}\right]\end{aligned} \tag{4.35}$$

in agreement with Eqs. (A3) and (A6) of Ref. 8. If one makes use of the series expansion of the Legendre polynomials, one obtains to lowest order in κ (see also Eq. (4.37)),

$$\left(b_{\ell\ell}^{00}\right)_{\text{stat}} = a'_\ell \kappa^{\ell/2} + \mathcal{O}(\kappa^{1+\ell/2}) \tag{4.36}$$

with coefficients a'_ℓ given explicitly by Eq. (B.3) of Appendix B in terms of hypergeometric functions. One has $a'_2 = 2\sqrt{5}/15$, $a'_4 = 4/105$, $a'_6 = 8\sqrt{13}/9009$. For the special case of vanishing external field, $h = 0$, the $\left(b_{\ell\ell}^{00}\right)_{\text{stat}}$ are the only non-vanishing stationary moments.

The remaining stationary moments of relevance for the general case of $h \neq 0$ and $\kappa \neq 0$ cannot be calculated analytically, but we can perform a Taylor expansion in both h and κ about $h = \kappa = 0$ to find

$$\left(b_{l_1 l_2}^{LM}\right)_{\text{stat}} \propto h^L \kappa^{l_2/2} \delta_{M,0} \quad (\text{even } l_2) \tag{4.37}$$

for even l_2, while for odd l_2 the moments vanish. The proportionality (4.37) can tediously be proven by direct integration of the stationary distribution function, or alternatively, upon inspecting the couplings between moments in the presence of non-vanishing h or κ. In particular does the contribution $\mathbf{C}_{\text{Bh}}$, entering with prefactor h in $\mathbf{A}$, when applied to $\mathbf{b}$, preserve l_2 and M, while L is either decreased or increased by 1. Same for $\mathbf{C}_{\text{Dh}}$. The action of $\mathbf{C}_{\text{D}\kappa}$ on $\mathbf{b}$ however preserves L and M, while changing l_2 by $+2$, 0, or -2.

As Eq. (4.35) is the stationary solution for any h and κ, this implies $\left[(\mathbf{C}_{\text{Dh}} \cdot \mathbf{b})_{22}^{00}\right]_{\text{stat}} = 0$, or equivalently,

$$\left(b_{32}^{10}\right)_{\text{stat}} = -\sqrt{\frac{3}{2}}\left(b_{12}^{10}\right)_{\text{stat}} \tag{4.38}$$

for any h and κ. Similarly, the stationary solution (4.25) fulfills $(\mathbf{A}\cdot\mathbf{b}_{\text{stat}} - \mathbf{d})_{10}^{10} = 0$ for $\kappa = 0$, i.e. without the $\mathbf{C}_{\text{D}\sigma}$ term. And again, if (4.25) is indeed the stationary solution for any h and κ, this implies $\left[(\mathbf{C}_{\text{D}\kappa} \cdot \mathbf{b})_{10}^{10}\right]_{\text{stat}} = 0$, or equivalently, confirms Eq. (4.38) for any h and κ, Moreover, Eq. (4.38) can also be inferred from (4.37) by matching powers of h and κ in the stationary state. To lowest order we have $\left(b_{32}^{10}\right)_{\text{stat}} = -2h\kappa/15 + \mathcal{O}(h\kappa^2)$ but also $\left(b_{22}^{00}\right)_{\text{stat}} \propto h^0[\kappa^1 + \mathcal{O}(\kappa^2)]$, $\left(b_{44}^{00}\right)_{\text{stat}} \propto h^0[\kappa^2 + \mathcal{O}(\kappa^4)]$, both independent of h, whereas $\left(b_{12}^{10}\right)_{\text{stat}} \propto (b_{32}^{10})_{\text{stat}} \propto [h^1 + \mathcal{O}(h^2)][\kappa^1 + \mathcal{O}(\kappa^2)]$. Since the latter two correspond to $L = 1$, the corresponding moment has to vanish according to (4.37) and therefore both contributions need to cancel each other. The equality (4.38) rules out l_1 to appear in the exponent of h or κ in Eq. (4.37).

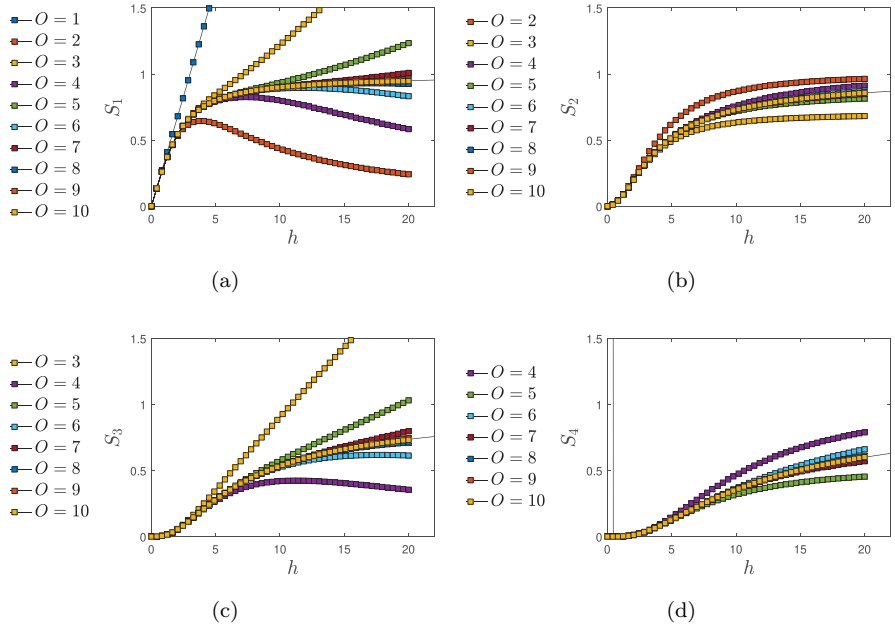

Fig. 2. (Color online) Order parameter $S_\ell = \langle P_\ell(\mathbf{e} \cdot \mathbf{e}_z)\rangle_{\text{stat}}$ defined by (4.25), or equivalently, reduced stationary moment $\left(b_{\ell 0}^{\ell 0}\right)_{\text{stat}}/\sqrt{2\ell+1}$ evaluated using different orders $O \geq \ell$. This order parameter depends on h only. The four panels show (a) $\ell = 1$, (b) $\ell = 2$, (c) $\ell = 3$ and (d) $\ell = 4$. Exact result (4.26): solid black.

4.3. *Limitation of the moment expansion*

Stationary moments obtained via matrix inversion, $\mathbf{b}^{\text{stat}} = \mathbf{A}^{-1} \cdot \mathbf{d}$, for several orders O of the expansion are compared with the exact stationary moments in Figs. 2 and 3. Up to moderate field strengths and anisotropy constants, we observe rapid convergence of our numerical results with increasing O towards the exact results. For $h \gtrsim 10$ or $\kappa \gtrsim 10$, however, higher order terms in the expansion ($O > 8$) need to be included in order to accurately recover the exact results.

Truncating the infinite sum in the expansion (4.3) to a finite number of terms, non-negativity of the probability density F is no longer guaranteed, which can lead to unphysical results. Therefore, we investigated the limits of validity of truncating the series to a finite order O by determining the threshold values h_{thres} and κ_{thres} beyond which non-negativity of the stationary F is violated.

Figure 4 shows that the threshold values h_{thres} and κ_{thres} increase only mildly with the order O of the expansion. On the other hand, the number of terms in the expansion grows rapidly with O, Eq. (3.6), implying that the numerical scheme becomes intractable especially for larger anisotropy constants. If one is interested in the magnetization $\propto b_{10}^{10}$, $O = 8$ is needed to obtain precise results for all $h \leq 20$ and $\kappa \leq 8$.

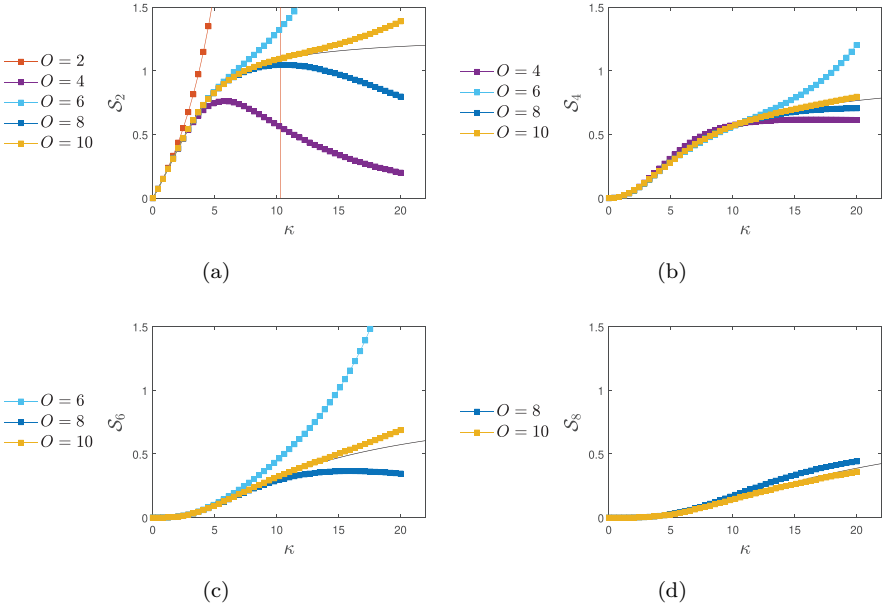

Fig. 3. (Color online) Order parameter $\mathcal{S}_\ell = \langle P_\ell(\mathbf{e}\cdot\mathbf{n})\rangle_{\text{stat}}$ defined by Eq. (4.32), or equivalently, reduced stationary moment $\left(b^{00}_{\ell\ell}\right)_{\text{stat}}/\sqrt{2\ell+1}$ evaluated using different orders $O \geq \ell$. These order parameters depend on κ only. The four panels show (a) $\ell = 2$, (b) $\ell = 4$, (c) $\ell = 6$ and (d) $\ell = 8$, as the odd order parameters S_ℓ vanish. The exact result (4.33) is shown as solid black lines.

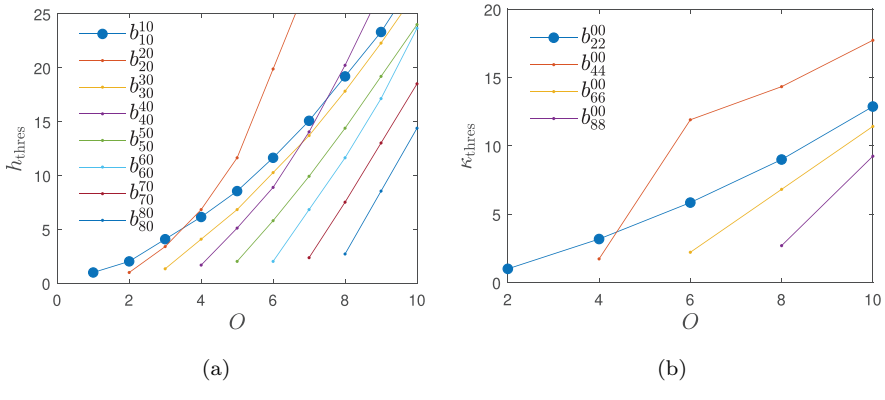

Fig. 4. (Color online) (a) Threshold h_{thres} value versus order O. Below h_{thres} the absolute relative deviation between exact and FP-generated stationary moment $b^{\mu 0}_{\mu 0}$ remains below 2%. (b) Same as (a) for moments $b^{00}_{\mu\mu}$. Here, the threshold κ_{thres} is plotted.

4.4. *Dynamical evolution in the presence of a stationary external field*

So far we explored the stationary moments in the presence of a stationary external field $h = h_0$. Using the known time-independent matrix $\mathbf{A}$ and constant vector $\mathbf{d}$,

as well as an initial probability density characterized by its moments $\mathbf{b}(0)$ at time zero, the solution of the system of linear differential equations (4.15) is given by

$$\begin{aligned}\mathbf{b}(t) &= e^{-\mathbf{A}t}\cdot\mathbf{b}(0) + \int_0^t e^{-\mathbf{A}t'}dt'\cdot\mathbf{d} \\ &= \mathbf{S}^{-1}\cdot\left[e^{-\mathbf{\Lambda}t}\cdot\mathbf{S}\cdot\mathbf{b}(0) + \int_0^t e^{-\mathbf{\Lambda}t'}dt'\cdot\mathbf{S}\cdot\mathbf{d}\right]\end{aligned} \tag{4.39}$$

or in components

$$b_K(t) = \sum_{\mu,\nu=1}^{I(n)-1} S^{-1}_{K\mu}\left[e^{-\lambda_\mu t}S_{\mu\nu}b_\nu(0) + \frac{1-e^{-\lambda_\mu t}}{\lambda_\mu}S_{\mu\nu}d_\nu\right], \tag{4.40}$$

where $\mathbf{S}^{-1}$ contains eigenvectors of $\mathbf{A}$ in its columns, $\mathbf{\Lambda}$ all the corresponding eigenvalues (λ's) on its diagonal. The longest relaxation time thus corresponds to the largest inverse eigenvalue, while all eigenvalues are positive within the range of applicability of the moment expansion approach.

In Fig. 5, the solution (4.40) is shown for some K and different orders O of the expansion. Panels (a) and (b) correspond to independent isotropic initial conditions, whereas in (c) the additional condition $\mathbf{e} = \mathbf{n}$ was enforced. For the chosen parameters, we observe a near-exponential behavior and a rather quick convergence with increasing order O of the expansion. For comparison, we provide analytical results for a low-order expansion in Appendix F. Horizontal dashed lines indicate the exactly known stationary values (4.35) and we confirm that the dynamical solutions approach the stationary value for long enough times. We also include in Fig. 5 the corresponding results of Brownian Dynamics (BD) simulations of the stochastic differential equations as described in Sec. 3.2. While both methods ultimately give the same results, we find that our solutions to the FP equation converge much more quickly compared to the stochastic simulations within the parameter range identified in Sec. 4.3. The computational effort is indeed very different for the two approaches. The time to compute $O = 10$ for the FP approach is roughly the same as $N = 100$ for the BD simulation, corresponding to a much lower precision. Note that the computing time for BD simulations scale as N, with the error decreasing very slowly as $1/\sqrt{N}$.

4.5. *Oscillating external field, susceptibility*

Next we consider an oscillating external field with strength $h = h_0 + h_1 e^{i\omega t}$ with small amplitude $|h_1| \ll 1$. The dynamical equation of change (4.15) reads

$$\dot{\mathbf{b}} = -\mathbf{A}(h)\cdot\mathbf{b} + \mathbf{d}(h), \tag{4.41}$$

where we highlight, for the present purpose, the dependency of $\mathbf{A}$ and $\mathbf{d}$ on h; both depend on the remaining parameters as well. For small amplitudes h_1, we can

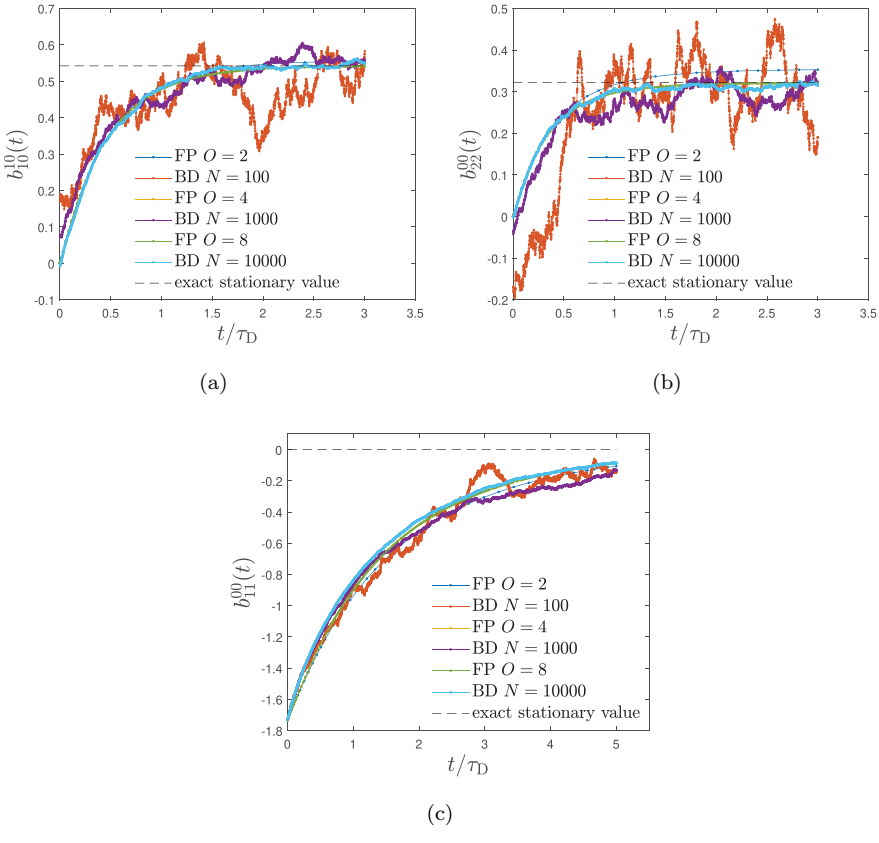

Fig. 5. (Color online) Transient dynamics of moments (a) $b_{10}^{10}(t)$, (b) $b_{22}^{00}(t)$ and (c) $b_{11}^{00}(t)$ in the presence of an external field $h = 1$ are shown. Isotropic initial condition is chosen in panels (a) and (b), while the initial configuration has isotropic $\mathbf{e}$ and $\mathbf{n} = \mathbf{e}$ in panel (c). Other parameters are chosen as $\tau_B/\tau_D = \kappa = 1$. Solutions to the FP equation for different orders O of the expansion are shown together with results of BD simulations for different number of realizations N. Horizontal dashed lines indicate the exactly known stationary value.

Taylor-expand $\mathbf{A}$ and $\mathbf{d}$ about $h = h_0$. If we furthermore introduce the frequency-dependent, complex amplitude of the oscillating deviation $\delta\mathbf{b}(\omega)$ from the stationary solution,

$$\delta\mathbf{b}(\omega)e^{i\omega t} = \mathbf{b}(t) - \mathbf{b}_{\text{stat}}(h_0), \tag{4.42}$$

we can plug this expression into (4.41) to obtain

$$\begin{aligned} i\omega\delta\mathbf{b} &= -\big[\mathbf{A}(h_0) + h_1\mathbf{A}'(h_0)\big]\big[\mathbf{b}_{\text{stat}}(h_0) + \delta\mathbf{b}\big] + \mathbf{d}(h) \\ &\approx -h_1\mathbf{A}'(h_0)\mathbf{b}_{\text{stat}}(h_0) - \mathbf{A}(h_0)\delta\mathbf{b} + h_1\mathbf{d}'(h_0) \end{aligned} \tag{4.43}$$

up to terms quadratic in h_1, and the prime denotes a derivative with respect to h. This equation is readily solved for $\delta\mathbf{b}(\omega)$ as

$$\delta\mathbf{b}(\omega) = h_1[\mathbf{A}(h_0) + i\omega\mathbf{1}]^{-1} \cdot \tilde{\mathbf{d}}, \tag{4.44}$$

where $\tilde{\mathbf{d}}$ is given according to as (4.43)

$$\tilde{\mathbf{d}} = -\mathbf{A}'(h_0)\cdot\mathbf{A}^{-1}(h_0)\cdot\mathbf{d}(h_0) + \mathbf{d}'(h_0). \tag{4.45}$$

So far the treatment is the general result within linear response theory, as we have not used any particular properties of $\mathbf{A}$ and $\mathbf{d}$. For the present work, $\mathbf{A}(h)$ and $\mathbf{d}(h)$ are both linear in h, so that $\mathbf{A}'(h_0) = \mathbf{A}'$ and $\mathbf{d}'(h_0) = \mathbf{d}'$ are constants independent on h_0, and thus $h_0\mathbf{d}' = \mathbf{d}(h_0) - \mathbf{d}(0)$ and $h_0\mathbf{A}' = \mathbf{A}(h_0) - \mathbf{A}(0)$, leading to

$$\begin{aligned} h_0\tilde{\mathbf{d}} &= \big[-h_0\mathbf{A}'\cdot\mathbf{A}^{-1}(h_0) + \mathbf{I}\big]\cdot\mathbf{d}(h_0) - \mathbf{d}(0) \\ &= \mathbf{A}(0)\cdot\mathbf{b}_{\text{stat}}(h_0) - \mathbf{d}(0), \end{aligned} \tag{4.46}$$

so that we finally have (assuming $h_0 > 0$)

$$\delta\mathbf{b}(\omega) = \frac{h_1}{h_0}[\mathbf{A}(h_0) + i\omega\mathbf{1}]^{-1}\cdot[\mathbf{A}(0)\cdot\mathbf{b}_{\text{stat}}(h_0) - \mathbf{d}(0)]. \tag{4.47}$$

If we know the eigensystem of $\mathbf{A}$, there is no need to invert a matrix for each ω separately. With $\delta\mathbf{b}(\omega)$ at hand, we have access to parallel susceptibilities of all moments, since dimensionless susceptibilities are proportional to $\delta\mathbf{b}(\omega)/h_1$. We can explicitly express the linear response relation between applied field and resulting parallel magnetization in Fourier-space as

$$\langle\mathbf{e}\cdot\mathbf{e}_z\rangle(\omega) = \mathcal{L}(h_0) + \frac{1}{3}\chi_\parallel^*(\omega)h_1(\omega), \tag{4.48}$$

where $\chi_\parallel^* = \chi_\parallel/\chi_{\text{L}}$ with the Langevin susceptibility $\chi_{\text{L}} = nm^2/(3k_{\text{B}}T)$. Using the expansion of the probability density into bipolar spherical harmonics, we can express this, with the help of $\langle\mathbf{e}\cdot\mathbf{e}_z\rangle = b_{10}^{10}/\sqrt{3}$, Eq. (4.48), as

$$\chi_\parallel^*(\omega) = \frac{\sqrt{3}}{h_1}\delta b_{10}^{10}(\omega). \tag{4.49}$$

Special case $h_0 = 0$. For the special case of $h_0 = 0$, Eq. (4.44) with Eq. (4.45) simplifies to

$$\delta\mathbf{b}(\omega) = h_1[\mathbf{A}(0) + i\omega\mathbf{1}]^{-1}\cdot\big[-\mathbf{A}'\cdot\mathbf{b}_{\text{stat}}(0) + \mathbf{d}'\big]. \tag{4.50}$$

Note that the only non-vanishing components of $\mathbf{b}_{\text{stat}}(0)$ are the known $\big(b_{\mu\mu}^{00}\big)_{\text{stat}}$ components, and that the only non-vanishing component of $\mathbf{d}'$ is its $^{10}_{10}$ component,

$$d'_K = \frac{1}{\sqrt{3}\tau_0}\delta_{K,{}^{10}_{10}}, \tag{4.51}$$

according to Eq. (4.16), because the prime stands for a derivative with respect to h.

Special case $\kappa = 0$. For the special case of $\kappa = 0$, $\mathbf{d}(0)$ vanishes, and $\mathbf{A}(0) = \boldsymbol{\tau}^{-1}$ is diagonal according to Eq. (4.17). Hence, due to Eq. (4.47),

$$\delta\mathbf{b}(\omega) = \frac{h_1}{h_0}\boldsymbol{\tau}^{-1}\cdot[\mathbf{A}(h_0) + i\omega\mathbf{1}]^{-1}\cdot\mathbf{b}_{\text{stat}}(h_0). \tag{4.52}$$

Note that for $\kappa = 0$ the only non-vanishing components of $\mathbf{b}_{\text{stat}}(h_0)$ are the known $\big(b_{\mu0}^{\mu0}\big)_{\text{stat}}$ components.

Special case $h_0 = \kappa = 0$. For this special case $\mathbf{A}(0) = \boldsymbol{\tau}^{-1}$, $\mathbf{b}_{\text{stat}} = \mathbf{0}$ and thus $\tilde{\mathbf{d}} = \mathbf{d}'$ so that Eq. (4.44) simplifies to $\delta\mathbf{b}(\omega) = h_1(\boldsymbol{\tau}^{-1} + i\omega\mathbf{I})^{-1}\cdot\mathbf{d}'$. Because $\mathbf{d}'$ has a single non-vanishing $^{10}_{10}$ component (4.51), and because $\left[\tau_{10}^{10}\right]^{-1} = \tau_{\text{B}}^{-1} + \tau_{\text{D}}^{-1} \equiv \tau_0^{-1}$, the only non-vanishing component of $\delta\mathbf{b}$ is

$$\delta b_{10}^{10}(\omega) = \frac{h_1}{\sqrt{3}} \frac{1}{(1 + i\omega\tau_0)}, \tag{4.53}$$

i.e. as expected, a simple Debye law with the effective relaxation time τ_0 for the case of vanishing anisotropy energy and external field.

Figure 6 shows the real and imaginary part of the reduced susceptibility $\chi_{\parallel}^*$, Eq. (4.49), for different values of h_0, κ and ratios $\tau_{\text{B}}/\tau_{\text{D}}$. For not too large values of $\tau_{\text{B}}/\tau_{\text{D}}$ and κ, we find that our numerical results are well described by the approximate Debye formula[19]

$$\chi_{\parallel}^*(\omega) \approx c \left[\frac{B}{1 + i\omega\tau_{\text{eff}}} + (1 - B) \right], \tag{4.54}$$

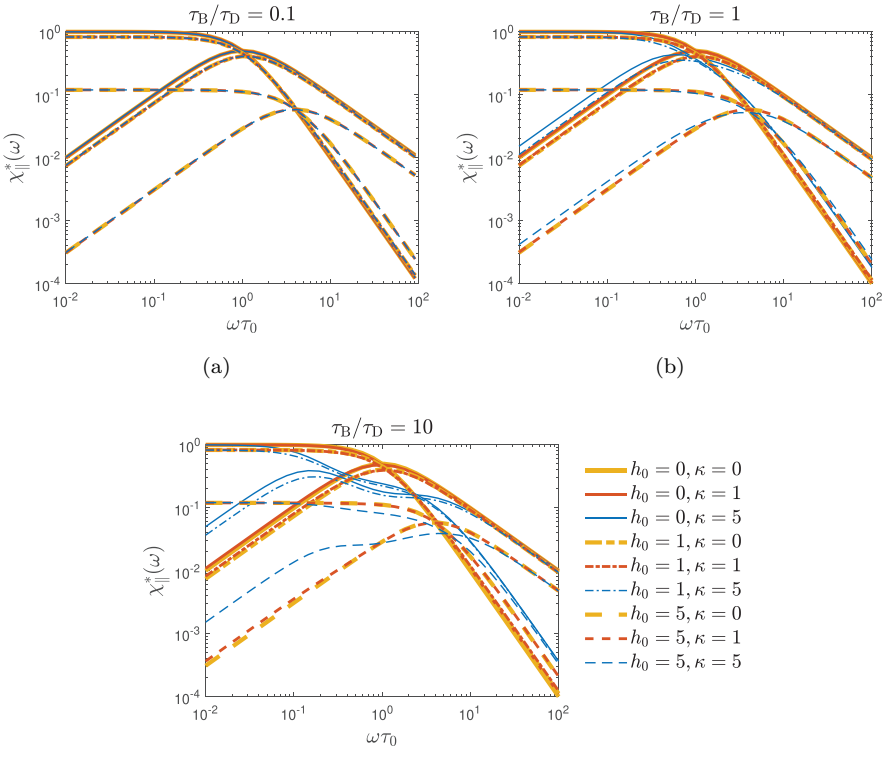

Fig. 6. (Color online) Real and imaginary parts of the complex susceptibility $\chi_{\parallel}^*(\omega)$ defined by Eq. (4.49) as a function of scaled frequency. The different panels (a)–(c) show different values of the ratio of relaxation times $\tau_{\text{B}}/\tau_{\text{D}}$, while each panel shows results for different values of h_0 and κ.

where c and B are field- and anisotropy-dependent coefficients. We note that in these parameter ranges good fits to Eq. (4.54) are obtained for $B \approx 1$, i.e. a simple Debye law. The effective relaxation time is defined by $\tau_{\text{eff}}^{-1} = \tau_{\text{B}}^{-1} + \tau_{\text{N}}^{-1}$, where τ_{N} denotes the Néel relaxation time corresponding to κ. Note that analytical expressions for c, B, τ_{eff} are given in Ref. 19. Good agreement between fits to Eq. (4.54) and numerical results was also reported in Ref. 17. However, we see clear deviations between our numerical results and the simple fit (4.54) for $\tau_{\text{B}}/\tau_{\text{D}} = 10$ due to the appearance of a double-peak structure. Therefore, we can confirm the conclusion reached in Ref. 25 (for a somewhat different model) that a single effective relaxation time τ_{eff} cannot account for the coupling of Brownian and Néel processes. However, this conclusion does not invalidate the approximate Debye formula (4.54), but rather restricts its range of validity.

4.6. *Spectrum of relaxation times*

As discussed above and mentioned also in Ref. 25, the coupled system of Brownian and Néel dynamics is not fully described by a single effective relaxation time. Therefore, we show in Fig. 7 the whole spectrum of inverse relaxation times for selected parameter values. The spectrum is obtained from the eigenvalues of the matrix $\mathbf{A}$ defined in Eq. (4.17). We note in passing that the zero eigenvalue of the Fokker–Planck equation (here absorbed in $\mathbf{d}$) corresponds to the equilibrium state. For $h = \kappa = 1$, we find that the smallest eigenvalue is $\lambda_{\text{min}} \approx 0.55\tau_{\text{D}}^{-1}$ (for $\tau_{\text{B}} = \tau_{\text{D}}$) and $0.095\tau_{\text{D}}^{-1}$ (for $\tau_{\text{B}} = 10\tau_{\text{D}}$). Since the longest relaxation time is given

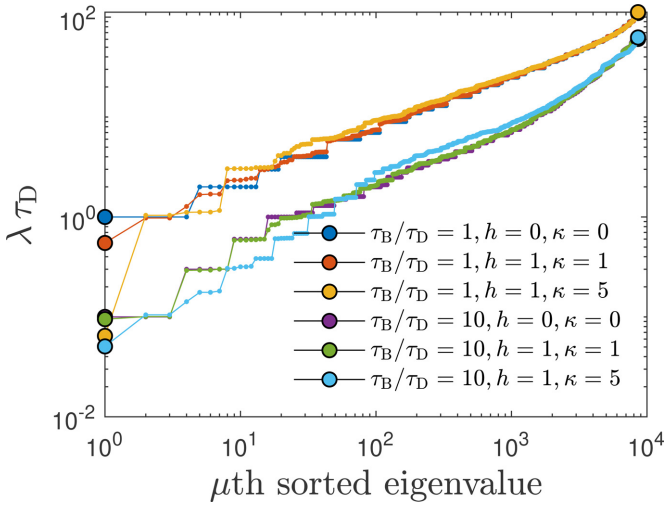

Fig. 7. (Color online) Spectrum of sorted eigenvalues λ_μ (multiplied by τ_{D}) versus μ for two different $\tau_{\text{B}}/\tau_{\text{D}}$ and various combinations of h and κ. There are $I(10) - 1 = 8590$ non-zero eigenvalues present in the shown spectrum that one obtains by diagonalizing $\mathbf{A}$ for $O = 10$. For $h = \kappa = 0$ one has $\mathbf{A} = \boldsymbol{\tau}^{-1}$ according to (4.17) and the eigenvalues and their degeneracies are given analytically by Eq. (4.13).

by the inverse of the smallest eigenvalues, we find that $\lambda_{\min}$ is approximately given by $1/\tau_{\mathrm{B}}$ when Brownian relaxation is significantly slower than τ_{D} (which applies to most magnetic nanoparticles). For comparison, we show in Fig. 7 also the spectrum in the uncoupled case ($h = \kappa = 0$), given by Eq. (4.13). In the uncoupled case, we find $\tau_{01}^{1M} = \tau_{\mathrm{B}}$ (three-fold degenerate due to $M = -1, 0, 1$) and $\tau_{11}^{00} = \tau_{\mathrm{D}}$, which corresponds to the second and third smallest eigenvalue for $\tau_{\mathrm{D}} = \tau_{\mathrm{B}} = 1$. Due to the coupling, a smaller eigenvalue, i.e. a larger relaxation time emerges. For $\tau_{\mathrm{B}} = 10\tau_{\mathrm{D}}$, the longest relaxation time is approximately given by $\tau_{01}^{1M} = \tau_{\mathrm{B}}$ (again three-fold degenerate). Coupling of Brownian and Néel processes leads in this case to the appearance of intermediate relaxation times between τ_{B} and τ_{D}.

The spectrum shown in Fig. 7 consists of all the eigenvalues of the matrix $\mathbf{A}$. However, not all of them are equally relevant for observables of interest. To discuss their relevance, let us rewrite Eq. (4.40) for the case of isotropic initial conditions as

$$b_K(t) = \sum_{\mu} w_{K\mu}[1 - e^{-\lambda_\mu t}] \tag{4.55}$$

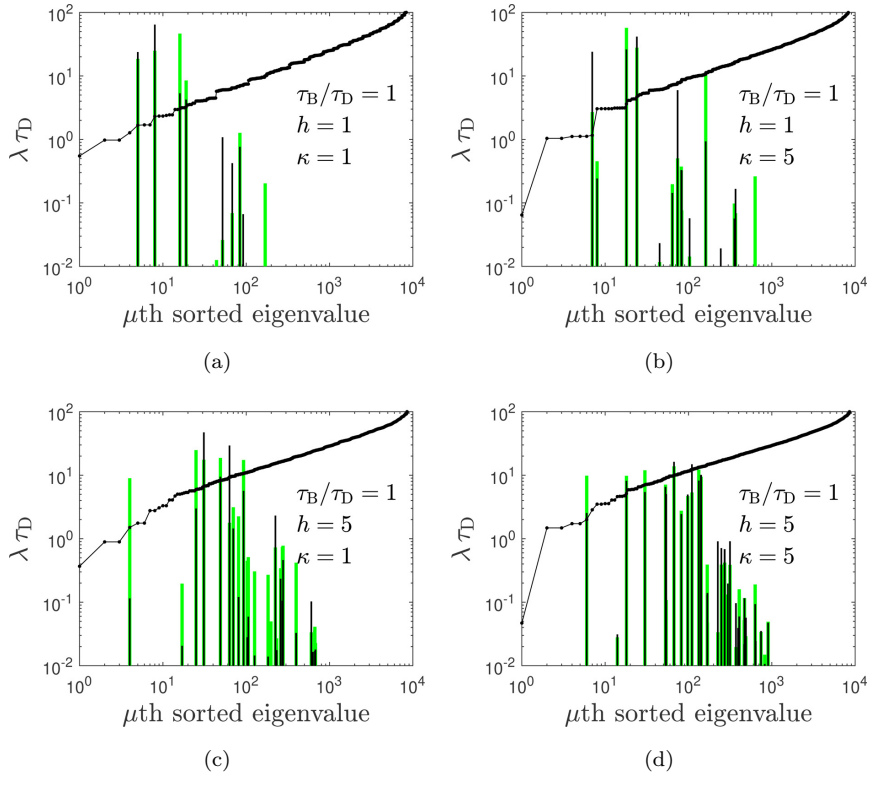

Fig. 8. (Color online) Relevance of the eigenvectors/eigenvalues (using $O = 10$). Eigenvalues λ_μ (black circles) shown together with their relative weights $|w_{K\mu}|$, defined by Eq. (4.56), for various combinations of model parameters h and κ at $\tau_{\mathrm{B}}/\tau_{\mathrm{D}} = 1$. Weights are normalized so that the sum over all weights is 100. Weights shown for two components, $K = {}^{10}_{10}$ (black) and $K = {}^{00}_{22}$ (green).

with

$$w_{K\mu} = S^{-1}_{K\mu}\lambda^{-1}_{\mu}\sum_{\nu} S_{\mu\nu}d_{\nu} = S^{-1}_{K\mu}\lambda^{-1}_{\mu}\left[S_{\mu,{}^{10}_{10}}d^{10}_{10} + S_{\mu,{}^{00}_{22}}d^{00}_{22}\right], \tag{4.56}$$

where the eigenvectors of $\mathbf{A}$ are the columns of the matrix $\mathbf{S}^{-1}$ in Eq. (4.40). We refer to $|w_{K\mu}|$ as the (time-independent) weight of eigenvector μ to b_K. In Fig. 8 we show the sorted eigenvalues together with their weights (percentage units) for the magnetization, $K = {}^{10}_{10}$, (black) and $K = {}^{00}_{22}$ (green vertical lines). It is remarkable to observe that up to moderate values of h and κ the weights are mostly concentrated on a few, nearby eigenvalues only. This finding helps to explain the near-exponential behavior and near-Debye susceptibility found earlier. We also note that the lowest eigenvalue carries a vanishing weight for the cases considered in Fig. 8 and therefore does not contribute to the magnetization dynamics. We can trace back many of the vanishing weights to the reduction in the non-vanishing coefficients b_K that significantly reduce from the total number (3.6) down to (E.1) when isotropic initial conditions are considered, see Appendix E.

5. Conclusions

We here consider the fundamental model for the rotational dynamics of magnetic nanoparticles proposed by Shliomis and Stepanov.[23,24] Although it is widely recognized that this model provides a physically sound starting point for studying such systems, the model is not widely used to date.[20] This finding is surprising given the growing interest in various applications and can partially be attributed to the rather complicated and numerically expensive solution of the model. Here, we follow recent works[17] and consider solutions to the underlying Fokker–Planck equation through an expansion in bipolar harmonics. While previous expressions were rather cumbersome, we here provide concise expressions for the resulting differential equations as well as numerical data that allow readers to readily implement the model (Appendix H). We test and validate our implementation for several limiting cases against analytical solutions as well as reference stochastic simulations. We also provide a discussion on convergence behavior and determine limits of applicability in terms of model parameters, beyond which the numerical scheme becomes unworkable due to the strongly growing number of degrees of freedom. Within the limits of applicability, we find the numerical scheme to be much more efficient than BD simulations of the corresponding stochastic differential equations. We also determine the full spectrum of relaxation times and find that only a relatively small subset is relevant for the magnetization dynamics.

Since we provide the numerical data for a straightforward and efficient implementation of the egg model, we hope that a broad range of researchers will be in a position to study this basic model of magnetization dynamics in great detail and for a broad range of parameters. Extensions to models with energy functions U

involving other than Y_{10}^{10} and Y_{22}^{00} bipolar harmonics are straightforward with Appendix D at hand, and will lead to systems of linear differential equations, whose ingredients enter the physical properties of the magnetic system in the presence of static and oscillating external fields, following the unaltered recipes provided in this work.

Appendix A. Examples for Rewriting Y_K in Terms of e and n

In Eqs. (3.8)–(3.9) we have expressed Y_{01}^{10} and Y_{10}^{10} in terms of $\mathbf{e}$, $\mathbf{n}$, and the basis vector $\mathbf{e}_z$. Here we provide some additional identities

$$\mathbf{n}\cdot\mathbf{e}_z = \frac{4\pi}{\sqrt{3}}Y_{01}^{10}, \tag{A.1}$$

$$\mathbf{n}\cdot\mathbf{e} = -\frac{4\pi}{\sqrt{3}}Y_{11}^{00}, \tag{A.2}$$

$$(\mathbf{n}\cdot\mathbf{e}_z)^2 - \frac{1}{3} = \frac{8\pi\sqrt{5}}{15}Y_{02}^{20}, \tag{A.3}$$

$$(\mathbf{e}\cdot\mathbf{e}_z)^2 - \frac{1}{3} = \frac{8\pi\sqrt{5}}{15}Y_{20}^{20}, \tag{A.4}$$

that help to interpret coupled equations of moments, as the corresponding identities for averages are simply obtained upon replacing $4\pi Y_K$ by b_K.

Appendix B. Modified Bessel Function, Proofs of Eqs. (4.31) and (4.36)

With the help of the polynomial coefficients of the modified spherical Bessel function of the first kind,[1]

$$I_\alpha(x) = \sum_{k=0}^{\infty} \frac{1}{k!\Gamma(k+\alpha+1)}\left(\frac{x}{2}\right)^{2k+\alpha}, \tag{B.1}$$

the leading term of the stationary moment $b_{\ell 0}^{\ell 0}$ is

$$\begin{aligned}\left(b_{\ell 0}^{\ell 0}\right)_{\text{stat}} &= \frac{\frac{\sqrt{2\ell+1}}{\Gamma(\ell+3/2)}\left(\frac{h}{2}\right)^{\ell+1/2}}{\frac{1}{\Gamma(3/2)}\left(\frac{h}{2}\right)^{1/2}} + O(h^{\ell+1}) \\ &= \frac{\sqrt{\pi(2\ell+1)}}{2\Gamma(\ell+3/2)}h^\ell + O(h^{\ell+1})\end{aligned} \tag{B.2}$$

thus proving the form of a_ℓ in (4.31). The corresponding expansion coefficient a'_ℓ required in (4.36) can be calculated as well.

$$a'_\ell = \frac{\sqrt{2\ell+1}}{2(l/2)!}\int_{-1}^{1} P_l(z)z^l\,dz$$

$$= \frac{2^\ell\sqrt{2\ell+1}}{2(\ell/2)!}\sum_{k=0,1,..}^{\ell}\binom{\ell}{k}\binom{\frac{\ell+k-1}{2}}{\ell}\int_{-1}^{1}z^{\ell+k}dz$$

$$= \frac{2^\ell\sqrt{2\ell+1}}{2(\ell/2)!}\sum_{k=0,2,..}^{\ell}\binom{\ell}{k}\binom{\frac{\ell+k-1}{2}}{\ell}\frac{2}{\ell+k+1}$$

$$= \frac{\sqrt{\pi(2\ell+1)}\,{}_pF_q\left(\left\{\frac{\ell+1}{2},\frac{\ell+1}{2},-\frac{\ell}{2}\right\},\left\{\frac{1}{2},\frac{\ell+3}{2}\right\},1\right)}{(\ell+1)[(\ell/2)!]^2\Gamma\left[\frac{1-\ell}{2}\right]} \tag{B.3}$$

involving the hypergeometric function ${}_pF_q$.[1,9]

Appendix C. Legendre Polynomials, Proofs of Eqs. (4.27), (4.33) and (4.34)

Let us quote three known identities for Legendre polynomials[1]

$$P'_{\ell+1}(x) = \sum_{k=\ell,\ell-2,..}^{0}(2k+1)P_k(x), \tag{C.1}$$

$$(2\ell+1)P_\ell(x) = P'_{\ell+1}(x) - P'_{\ell-1}(x), \tag{C.2}$$

$$(2\ell+1)xP_\ell(x) = (\ell+1)P_{\ell+1}(x) + \ell P_{\ell-1}(x), \tag{C.3}$$

where the prime denotes a derivative with respect to x. The identity (C.2) follows immediately from Eq. (C.1), and leads directly to the recurrence relation (4.27) between order parameters $S_\ell = \langle P_\ell(\mathbf{e}\cdot\mathbf{e}_z)\rangle_{\text{stat}}$ or the stationary moments $\left(b_{\ell 0}^{\ell 0}\right)_{\text{stat}} = \sqrt{2\ell+1}\,S_\ell$.

To prove (4.33) we recall the definition of $\mathcal{S}_\ell$

$$\mathcal{S}_\ell = \langle P_\ell(\mathbf{e}\cdot\mathbf{n})\rangle_{\text{stat}} = \frac{\int_{-1}^{1}P_\ell(z)e^{\kappa z^2}\,dz}{\mathcal{N}} \tag{C.4}$$

with a denominator $\mathcal{N}$ that evaluates to

$$\mathcal{N} = \int_{-1}^{1}e^{\kappa z^2}\,dz = \sqrt{\frac{\pi}{\kappa}}\text{erfi}\sqrt{\kappa} = \frac{2e^\kappa \text{Da}(\sqrt{\kappa})}{\sqrt{\kappa}}, \tag{C.5}$$

where it is common to replace the imaginary error function erfi by Dawson's function Da. Using the identity (C.3) one can write, with $u(x) = (2\ell+1)P_n(x)$, $v'(x) = xe^{\kappa x^2}$ and $v(x) = e^{\kappa x^2}/2\kappa$,

$$\int_{-1}^{1}\frac{uv'}{\mathcal{N}}dx = \frac{uv}{\mathcal{N}}\Big|_{-1}^{1} - \frac{(2\ell+1)}{2\kappa\mathcal{N}}\int_{-1}^{1}P'_\ell e^{\kappa x^2}dx$$

$$
\begin{aligned}
&= \frac{uv}{\mathcal{N}}\Big|_{-1}^{1} - \frac{(2\ell+1)}{2\kappa} \sum_{k=\ell-1,\ell-3,..}^{0} (2k+1)\mathcal{S}_k \\
&= (\ell+1)\mathcal{S}_{\ell+1} + \ell\mathcal{S}_{\ell-1}.
\end{aligned}
\tag{C.6}
$$

The yet unevaluated $uv|_{-1}^{1}$ vanishes for the less interesting case of even ℓ. For odd ℓ, one has

$$
uv|_{-1}^{1} = \frac{(2\ell+1)P_n(x)e^{\kappa x^2}}{2\kappa}\Big|_{-1}^{1} = \frac{(2\ell+1)e^{\kappa}}{\kappa}. \tag{C.7}
$$

Putting this together, and replacing ℓ by $\ell-1$, we end up with the recursive relationship for even $\ell \geq 2$,

$$
\mathcal{S}_\ell = \frac{(2\ell-1)}{2\kappa\ell}\left[\frac{2e^{\kappa}}{\mathcal{N}} - \sum_{k=1}^{\ell/2}(4k-3)\mathcal{S}_{2(k-1)}\right] - \frac{(\ell-1)\mathcal{S}_{\ell-2}}{\ell}, \tag{C.8}
$$

while $\mathcal{S}_0 = 1$. For example

$$
\begin{aligned}
\mathcal{S}_2 &= \frac{3}{4\kappa}\left[\frac{2e^{\kappa}}{\mathcal{N}} - \mathcal{S}_0\right] - \frac{\mathcal{S}_0}{2}, \\
\mathcal{S}_4 &= \frac{7}{8\kappa}\left[\frac{2e^{\kappa}}{\mathcal{N}} - \mathcal{S}_0 - 5\mathcal{S}_2\right] - \frac{3\mathcal{S}_2}{4}.
\end{aligned}
\tag{C.9}
$$

If we denote the square bracket in Eq. (C.8) by $Q(\ell)$, one has $Q(\ell+2) = Q(\ell) - (2\ell+1)\mathcal{S}_\ell$. Hence,

$$
\begin{aligned}
\mathcal{S}_{\ell+2} &= \frac{(2\ell+3)}{2\kappa(\ell+2)}Q(\ell+2) - \frac{(\ell+1)\mathcal{S}_\ell}{\ell+2} \\
&= \frac{(2\ell+3)}{2\kappa(\ell+2)}[Q(\ell) - 2(\ell+1)\mathcal{S}_\ell] - \frac{(\ell+1)\mathcal{S}_\ell}{\ell+2}
\end{aligned}
\tag{C.10}
$$

and $Q(\ell)$ can be expressed in terms of $\mathcal{S}_\ell$ and $\mathcal{S}_{\ell-2}$ via Eq. (C.8). This leads to Eq. (4.34).

Appendix D. Products of Bipolar Harmonics

The product of two bipolar harmonics can be written as[27]

$$
Y_{K'}Y_K = \sum_{L'',M''} C_{L'M'LM}^{L''M''} \sum_{l_1'',l_2''} B_{l_1'l_2'L'l_1l_2L}^{l_1''l_2''L''} Y_{l_1''l_2''}^{L''M''} \tag{D.1}
$$

with $\left|l_1'' - l_2''\right| \leq L'' \leq l_1'' + l_2''$ and $|M''| \leq L''$. In (D.1), the C's are Clebsch–Gordan coefficients and using $\tilde{x} = 2x + 1$, the B's are given in terms of Clebsch–Gordan coefficients and a Wigner's 9j-symbol $\{\ldots\}$ as

$$B^{l_1'' l_2'' L''}_{l_1' l_2' L' l_1 l_2 L} = \frac{\sqrt{\tilde{l}_1' \tilde{l}_2' \tilde{l}_1 \tilde{l}_2 \tilde{L} \tilde{L}'}}{4\pi} C^{l_1'' 0}_{l_1' 0 l_1 0} C^{l_2'' 0}_{l_2' 0 l_2 0} \begin{Bmatrix} l_1' & l_1 & l_1'' \\ l_2' & l_2 & l_2'' \\ L' & L & L'' \end{Bmatrix}. \tag{D.2}$$

The Wigner 9j symbols, in turn, are calculated using Wigner's 6j symbols[13]

$$\begin{Bmatrix} l_1' & l_1 & l_1'' \\ l_2' & l_2 & l_2'' \\ L' & L & L'' \end{Bmatrix} = \sum_{g=g_1}^{g_2} (-1)^{2g} (2g+1) \begin{Bmatrix} g & L'' & l_1' \\ l_1'' & l_1 & l_2'' \end{Bmatrix} \begin{Bmatrix} g & l_2' & L \\ l_2 & l_1 & l_2'' \end{Bmatrix} \begin{Bmatrix} g & L'' & l_1' \\ L' & l_2' & L \end{Bmatrix} \tag{D.3}$$

and the 6j-symbols can be calculated using the 3j-symbols. Due to symmetry properties of Wigner's 6j-symbols

$$\begin{Bmatrix} j_1 & j_2 & j_3 \\ j_4 & j_5 & j_6 \end{Bmatrix}, \tag{D.4}$$

that vanish except if $|j_2 - j_3| \leq j_1 \leq j_2 + j_3$, the sum in Eq. (D.3) runs from $g_1 = \max\left(|L'' - l_1'|, |L - l_2'|\right)$ to $g_2 = \min\left(L'' + l_1', L + l_2'\right)$.

For the special case of $K = {}^{10}_{10}$, in light of Eq. (3.14), all the non-zero terms in Eq. (D.1) are

$$Y_K Y^{10}_{10} = \sum_{L'=L-1}^{L+1} C^{L'M}_{LM10} \sum_{l_1'=l_1-1}^{l_1+1} B^{l_1' l_2 L'}_{l_1 l_2 L 101} Y^{L'M}_{l_1' l_2}, \tag{D.5}$$

where both sums are meant to extend over positive values of the summation indices only. Similarly, for the special case of $K = {}^{00}_{22}$, using Eq. (3.15), the non-zero terms of Eq. (D.1) are

$$Y_K Y^{00}_{22} = \sum_{l_1'=l_1-2}^{l_1+2} \sum_{l_2'=l_2-2}^{l_2+2} B^{l_1' l_2' L}_{l_1 l_2 L 220} Y^{LM}_{l_1' l_2'}, \tag{D.6}$$

where we made use of $C^{LM}_{LM00} = 1$, and where again both sums extend over positive values of the summation indices only. If one does not save the 9j symbols or B components, the computational effort scales with O^3 if we are interested in the coefficients $\mathcal{P}$ and $\mathcal{Q}$ up to some order O.

Appendix E. Number of Non-Zero Moments for Isotropic Initial Conditions

Provided the initial condition is isotropic, the number of non-zero moments and eigenvalues that can potentially contribute in Fig. 8 is given by

$$I_{\text{iso}}(O) = \sum_{l_1=0}^{O} \sum_{\substack{l_2=0 \\ \text{even}}}^{O} \sum_{L=|l_1-l_2|}^{\min(O,l_1+l_2)} 1$$
$$= \begin{cases} \left(\frac{1}{2} + \frac{3}{8}O + \frac{1}{4}O^2\right)(2+O) & \text{even } O, \\ \left(\frac{3}{8} + \frac{3}{8}O + \frac{1}{4}O^2\right)(1+O) & \text{odd } O, \end{cases} \tag{E.1}$$

because only multi-indices K with even l_2 and vanishing M can be reached, according to Eqs. (4.22) and (4.23). For the special case of $\kappa = 0$ this number is further reduced to

$$I_{\text{iso}}^{\kappa=0}(O) = \sum_{l_1=0}^{O} 1 = 1 + O \tag{E.2}$$

and for the special case of $h = 0$ one has

$$I_{\text{iso}}^{h=0}(O) = \sum_{\substack{l_1=0 \\ \text{even}}}^{O} \sum_{\substack{l_2=0 \\ \text{even}}}^{O} \sum_{L=|l_1-l_2|}^{\min(O,l_1+l_2)} 1$$
$$= \begin{cases} \left(\frac{1}{2} + \frac{1}{4}O + \frac{1}{8}O^2\right)(2+O) & \text{even } O, \\ \left(\frac{1}{4} + \frac{1}{8}O + \frac{1}{8}O^2\right)(1+O) & \text{odd } O. \end{cases} \tag{E.3}$$

Table 1. Number of non-zero moments for the Oth order expansion, including b_{00}^{00}, according to Eqs. (3.6), (E.1), (E.3), (E.2) and (E.4).

O	$I(O)$	$I_{\text{iso}}(O)$	$I_{\text{iso}}^{\kappa=0}(O)$	$I_{\text{iso}}^{h=0}(O)$	$I^{M=0}(O)$
1	11	2	2	1	5
2	51	9	3	6	15
3	156	15	4	7	34
4	375	36	5	21	65
5	771	51	6	24	111
6	1421	94	7	52	175
7	2416	122	8	58	260
8	3861	195	9	105	369
9	5875	240	10	115	505
10	8591	351	11	186	671
20	113,631	2376	21	1221	4641
50	3,947,451	33,501	51	16,926	66,351

These numbers are small compared with the total number $I(O)$ given by (3.6). For large O, $I_{\text{iso}}(O)/I(O) = 3O^{-1}/7$. As the number of available moments with $M = 0$ is

$$I^{M=0}(O) = \sum_{l_1=0}^{O} \sum_{l_2=0}^{O} \sum_{L=|l_1-l_2|}^{\min(O,l_1+l_2)} 1 = \left(1 + O + \frac{1}{2}O^2\right)(1+O), \tag{E.4}$$

basically half of the set of moments with $M = 0$ is non-zero for isotropic initial conditions. Explicit values for the various amounts are provided in Table 1. The sums have been evaluated analytically by equating a polynomial in O with unknown coefficients to exactly enumerated numbers.

Appendix F. Low-Order Expansion Around Isotropic State

Consider isotropic initial conditions $F(\mathbf{e}, \mathbf{n}) = (4\pi)^{-2}$ at $t = 0$. Take into account all moments $b^{L,M}_{l_1,l_2}$ up to $l_1 = l_2 = L = |M| = O$ with $O = 1$, and set all remaining ones to zero. In view of Eq. (4.37), this approximation applies for $h \ll 1$ and $\kappa = 0$. In accord with Appendix E, there is just a single nontrivial equation of change. It reads

$$\dot{b}^{10}_{10} = -\frac{(\tau_{\text{B}} + \tau_{\text{D}})\left(u_h + 4\pi b^{10}_{10}\right)}{4\pi\tau_{\text{B}}\tau_{\text{D}}}. \tag{F.1}$$

The solution of the whole system of equations is

$$\langle \mathbf{e} \cdot \mathbf{e}_z \rangle = \frac{b^{10}_{10}}{\sqrt{3}} = \frac{(1 - e^{-t/\tau_0})h}{3}, \tag{F.2}$$

$$\langle \mathbf{e} \cdot \mathbf{n} \rangle = -\frac{b^{00}_{11}}{\sqrt{3}} = 0, \tag{F.3}$$

$$\langle \mathbf{n} \cdot \mathbf{e}_z \rangle = \frac{b^{10}_{01}}{\sqrt{3}} = 0. \tag{F.4}$$

This set of equations correctly captures the lowest order Taylor expansion in h. Including higher order moments, the system of equations quickly becomes very lengthy. Proceeding numerically, the stationary value for $h = 1$ and $O = 1$ ($O = 2$, $O = 3$), is $b^{10}_{10} = 1/3$ (0.313029, 0.313008), to be compared with the exact value 0.313035. For $h = 10$, again for $O = 1$ ($O = 2$, $O = 3$, $O = 4$), the stationary value is $b^{10}_{10} = 10/3$ (0.428494, 1.2216, 0.799939), to be compared with the exact value 0.9, demonstrating again that the convergence behavior is poor for large values of h.

Consider now all moments up to $l_1, l_2 \leq 2$, $L = M = 0$. In this case, one obtains single-exponential relaxation

$$\dot{b}^{00}_{11} = -\frac{1}{\tau_{\text{D}}}\left(1 - \frac{2\kappa}{5}\right) b^{00}_{11},$$

$$\dot{b}^{00}_{22} = -\frac{1}{\tau_{\text{D}}}\left[\left(3 - \frac{2\kappa}{7}\right) b^{00}_{22} - \frac{2\kappa}{\sqrt{5}}\right]. \tag{F.5}$$

For isotropic initial configuration, the solution is

$$b_{22}^{00}(t) = \frac{14\kappa}{\sqrt{5}(21-2\kappa)}\left[1-\exp\left(-\frac{(21-2\kappa)t}{7\tau_{\mathrm{D}}}\right)\right]. \tag{F.6}$$

If one takes into account the $L=1$ terms in addition, b_{22}^{00} couples to b_{12}^{10} and b_{10}^{10} and the resulting system cannot be solved analytically anymore. For the number of non-zero moments up to order O for isotropic initial conditions see Appendix E.

Appendix G. Modified Egg Model

As mentioned above, Weizenecker[29] proposed a somewhat different model compared to the egg model of Shliomis and Stepanov. Here, we briefly discuss the corresponding changes in our treatment, if one were to use this model instead.

Assuming again that Larmor precession can be neglected, the difference between the models boils down to the use of the rotational operator $\boldsymbol{\mathcal{L}}_n$ instead of $\boldsymbol{\mathcal{L}}$ in Eqs. (2.3) and (4.7). Since bipolar harmonics are also eigenfunctions of $\boldsymbol{\mathcal{L}}_n$, see Eq. (4.8), we find that $\boldsymbol{\mathcal{L}}_n^2(\beta U) = -6u_\kappa Y_{22}^{00}$ to be compared to (4.9). Collecting the resulting terms, we find that Eq. (4.12) are replaced with

$$\begin{aligned}
\dot{b}_K = &-\frac{1}{\tau_K^{\mathrm{W}}} b_K \\
&+ \frac{u_h}{4\tau_{\mathrm{B}}} \sum_{K'} b_{K'}\left[l_2'(l_2'+1) - l_2(l_2+1)\right]\mathcal{P}_K^{K'} \\
&+ \frac{u_\kappa}{4\tau_{\mathrm{B}}} \sum_{K'} b_{K'}\left[l_2'(l_2'+1) - l_2(l_2+1) - 6\right]\mathcal{Q}_K^{K'} \\
&+ \frac{u_h}{4\tau_{\mathrm{D}}} \sum_{K'} b_{K'}\left[l_1'(l_1'+1) - l_1(l_1+1) - 2\right]\mathcal{P}_K^{K'} \\
&+ \frac{u_\kappa}{4\tau_{\mathrm{D}}} \sum_{K'} b_{K'}\left[l_1'(l_1'+1) - l_1(l_1+1) - 6\right]\mathcal{Q}_K^{K'}
\end{aligned} \tag{G.1}$$

with the relaxation times τ_K^{W},

$$\tau_K^{\mathrm{W}} = \left[\frac{l_2(l_2+1)}{2\tau_{\mathrm{B}}} + \frac{l_1(l_1+1)}{2\tau_{\mathrm{D}}}\right]^{-1}. \tag{G.2}$$

In full analogy with Eq. (4.15), we can write (G.1) as $\dot{\mathbf{b}} = -\mathbf{A}^{\mathrm{W}} \cdot \mathbf{b} + \mathbf{d}^{\mathrm{W}}$ with

$$\mathbf{A}^{\mathrm{W}} = \frac{u_h}{\tau_{\mathrm{B}}}\mathbf{C}_{\mathrm{Bh}}^{\mathrm{W}} + \frac{u_\kappa}{\tau_{\mathrm{B}}}\mathbf{C}_{\mathrm{B}\kappa}^{\mathrm{W}} + \frac{u_h}{\tau_{\mathrm{D}}}\mathbf{C}_{\mathrm{Dh}}^{\mathrm{W}} + \frac{u_\kappa}{\tau_{\mathrm{D}}}\mathbf{C}_{\mathrm{D}\kappa}^{\mathrm{W}} + (\boldsymbol{\tau}^{\mathrm{W}})^{-1}, \tag{G.3}$$

where $\boldsymbol{\tau}^{\mathrm{W}}$ is a diagonal matrix with diagonal components given by τ_K^{W}, cf. Eq. (G.2). The inhomogeneity is given by

$$d_K^{\mathrm{W}} = \frac{h}{\sqrt{3}\tau_{\mathrm{D}}}\delta_{K,{}_{10}^{10}} + \frac{2\kappa}{\sqrt{5}\tau_0}\delta_{K,{}_{22}^{00}} \tag{G.4}$$

and thus identical with (4.16) upon exchanging τ_0 and τ_D. All the constant matrices appearing in (G.3) that are sufficient to write down $\mathbf{A}^W$ are provided as part of our supplementary data up to $O = 10$ (Appendix H).

For the equations of change of the two particular moments b_{10}^{10} and b_{22}^{00} one obtains for Weizenecker's modified egg model

$$\dot{b}_{10}^{10} = -\frac{h}{\sqrt{15}\tau_D} b_{20}^{20} - \frac{2\kappa}{5\sqrt{3}\tau_D}\left(\sqrt{\frac{3}{2}} b_{12}^{10} + b_{32}^{10}\right) - \frac{1}{\tau_D} b_{10}^{10} + \frac{h}{\sqrt{3}\tau_D}, \tag{G.5}$$

$$\dot{b}_{22}^{00} = -\left(\frac{3}{\tau_0} - \frac{2\kappa}{7\tau_0}\right) b_{22}^{00} - \frac{8\kappa}{7\sqrt{5}\tau_0} b_{44}^{00} - \frac{h}{\sqrt{5}\tau_D}\left(\sqrt{\frac{3}{2}} b_{12}^{10} + b_{32}^{10}\right) + \frac{2\kappa}{\sqrt{5}\tau_0}. \tag{G.6}$$

For a better comparison, the original equations of change for the egg model according to (4.20) and (4.21) read

$$\dot{b}_{10}^{10} = -\frac{h}{\sqrt{15}\tau_0} b_{20}^{20} - \frac{2\kappa}{5\sqrt{3}\tau_D}\left(\sqrt{\frac{3}{2}} b_{12}^{10} + b_{32}^{10}\right) - \frac{1}{\tau_0} b_{10}^{10} + \frac{h}{\sqrt{3}\tau_0}, \tag{G.7}$$

$$\dot{b}_{22}^{00} = -\left(\frac{3}{\tau_D} - \frac{2\kappa}{7\tau_D}\right) b_{22}^{00} - \frac{8\kappa}{7\sqrt{5}\tau_D} b_{44}^{00} - \frac{h}{\sqrt{5}\tau_D}\left(\sqrt{\frac{3}{2}} b_{12}^{10} + b_{32}^{10}\right) + \frac{2\kappa}{\sqrt{5}\tau_D}. \tag{G.8}$$

For the special case of $h = \kappa = 0$, the relaxation of the magnetization is determined by τ_D and τ_0 for the versions proposed in Refs. 29 and 23, respectively.

Appendix H. Supplementary Data and Code

As part of this contribution we provide all the constant matrices and vectors of order $O \in \{1, 2, \ldots, 10\}$ required to build the sparse matrix $\mathbf{A}$ and the vector $\mathbf{d}$ for any chosen O, and for any set of model parameters via (4.17) for the case of the egg model, and via (G.3) for the case of the modified egg model. With $\mathbf{A}$ and $\mathbf{d}$ at hand the time evolution of all moments is given by $\dot{\mathbf{b}} = -\mathbf{A} \cdot \mathbf{b} + \mathbf{d}$ and the stationary moments are conveniently obtained via $\mathbf{b}_{\text{stat}} = \mathbf{A}^{-1} \cdot \mathbf{d}$, while is not actually necessary to invert matrix $\mathbf{A}$. We have chosen to save all sparse matrices using Matlab^{TM}'s binary format, other formats can be provided upon request from authors.

To be specific, for a given O, with $n = I(O) - 1$, all $n \times n$ matrices and n-vectors for the egg model are obtained via a single Matlab^{TM}

$$\texttt{load}(\text{“}\texttt{load-order-}O\texttt{.mat}\text{”}) \tag{H.1}$$

command. This command returns $n \times n$ sparse matrices `CB`, `CD`, `CBh`, `CDh`, `CDk`, n-vectors `dBh`, `dDh`, `dDk`, as well as a matrix `K` with n rows and four columns. The four columns l_1, l_2, L, M encode the multi-index K for each of the n moments. For any choice of model parameters τ_B, τ_D, u_h, u_κ, the sparse $n \times n$ matrix $\mathbf{A}$ is constructed via

$$\begin{aligned} \texttt{A} = @(\tau_B, \tau_D, u_h, u_\kappa)\ & u_h\texttt{CBh}/\tau_B + u_h\texttt{CDh}/\tau_D \\ & + u_\kappa\texttt{CDk}/\tau_D + \texttt{CB}/\tau_B + \texttt{CD}/\tau_D, \end{aligned} \tag{H.2}$$

where the last two contributions encode $\boldsymbol{\tau}^{-1}$, and where u_h and u_κ can also be written in terms of h and κ, cf. Eq. (4.2). Similarly, the vector $\mathbf{d}$ is constructed via

$$\mathtt{d} = @(\tau_\mathrm{B}, \tau_\mathrm{D}, u_h, u_\kappa)\ u_h\mathtt{dBh}/\tau_\mathrm{B} + u_h\mathtt{dDh}/\tau_\mathrm{D} + u_\kappa\mathtt{dDk}/\tau_\mathrm{D}. \tag{H.3}$$

This vector $\mathbf{d}$ has n components. The μth component corresponds to multi-index $\mathtt{K}(\mu,:)$. The n stationary moments collected in vector $\mathbf{b}_\mathrm{stat}$ are obtained via

$$\mathtt{bstat} = \mathtt{A}(\tau_\mathrm{B}, \tau_\mathrm{D}, u_h, u_\kappa)\backslash\mathtt{d}(\tau_\mathrm{B}, \tau_\mathrm{D}, u_h, u_\kappa). \tag{H.4}$$

Equations (H.1)–(H.4) constitute a complete code. If one prefers to have a function that returns the component number μ for given multi-index $K = {}^{LM}_{l_1 l_2}$, one can do the following:

$$\begin{aligned}\mathtt{mu} = @(l_1, l_2, L, M)\ \mathtt{find}((l_1{=}{=}\mathtt{K}(:,1))\\ \&(l_2{=}{=}\mathtt{K}(:,2))\&(L{=}{=}\mathtt{K}(:,3))\&(M{=}{=}\mathtt{K}(:,4))).\end{aligned} \tag{H.5}$$

The stationary moment $(b^{10}_{10})_\mathrm{stat}$ is then for example given by

$$\mathtt{bstat}(\mathtt{mu}(1,0,1,0)). \tag{H.6}$$

If one is interested in the full inverse $\mathbf{A}^{-1}$, one has to first convert the sparse matrix into a full matrix via $\mathtt{inv}(\mathtt{full}(\mathtt{A}))$. Eigenvalues are retrieved with the help of $\mathtt{eig}(\mathtt{A})$.

There are tiny modifications for Weizenecker's modified egg model (Appendix G). Instead of `load-order-`O`.mat` one has to load `load-order-`O`-W.mat`. And there are additional summands $u_\kappa\mathtt{CBk}/\tau_\mathrm{B}$ in (H.2) and $u_\kappa\mathtt{dBk}/\tau_\mathrm{B}$ in (H.3), in accord with (G.3). Otherwise, codes are identical.

Acknowledgments

This project was supported by the Swiss National Science Foundation (grant 200021L-185052). The authors thank the Swiss National Supercomputing Centre for providing computing resources (project s987).

References

1. M. Abramowitz and I. Stegun, *Handbook of Mathematical Functions* (Dover, 1964).
2. D. V. Berkov, N. L. Gorn, R. Schmitz and D. Stock, Langevin dynamic simulations of fast remagnetization processes in ferrofluids with internal magnetic degrees of freedom, *J. Phys. Condens. Matter* **18** (2006) S2595–S2621.
3. W. T. Coffey, P. J. Cregg and Y. P. Kalmykov, On the theory of Debye and Néel relaxation of single domain ferromagnetic particles, in *Advances in Chemical Physics*, Vol. 83, eds. I. Prigogine and S. A. Rice (John Wiley & Sons, 1993), pp. 263–464.
4. P. Degond and J.-G. Liu, Hydrodynamics of self-alignment interactions with precession and derivation of the Landau-Lifschitz-Gilbert equation, *Math. Models Methods Appl. Sci.* **22** (2012) 1140001.
5. J. L. Garcia-Palacios, *On the Statics and Dynamics of Magneto-Anisotropic Nanoparticles* (John Wiley & Sons, 2000).

6. S. Hess, *Tensors for Physics* (Springer International Publishing, 2015).
7. P. Ilg, Equilibrium magnetization and magnetization relaxation of multicore magnetic nanoparticles, *Phys. Rev. B* **95** (2017) 214427.
8. P. Ilg, Diffusion-jump model for the combined Brownian and Néel relaxation dynamics of ferrofluids in the presence of external fields and flow, *Phys. Rev. E* **100** (2019) 022608.
9. P. Ilg and M. Kröger, Dynamics of interacting magnetic nanoparticles: Effective behavior from competition between Brownian and Néel relaxation, *Phys. Chem. Chem. Phys.* **22** (2020) 22244–22259.
10. P. Ilg, M. Kröger and S. Hess, Magnetoviscosity and orientational order parameters of dilute ferrofluids, *J. Chem. Phys.* **116** (2002) 9078–9088.
11. S. H. L. Klapp, Dipolar fluids under external perturbations, *J. Phys. Condens. Matter* **17** (2005) R525–R550.
12. M. Kröger, A. Ammar and F. Chinesta, Consistent closure schemes for statistical models of anisotropic fluids, *J. Non-Newton. Fluid Mech.* **149** (2008) 40–55.
13. A. Messiah, '9j' symbols. Appendix C.III, in *Quantum Mechanics*, Vol. 2 (North-Holland, 1962).
14. R. H. Nochetto, A. J. Salgado and I. Tomas, The equations of ferrohydrodynamics: Modeling and numerical methods, *Math. Models Methods Appl. Sci.* **26** (2016) 2393–2449.
15. S. Odenbach (ed.), *Colloidal Magnetic Fluids*, Lecture Notes in Physics, Vol. 763 (Springer, 2009).
16. H. C. Öttinger, *Stochastic Processes in Polymeric Fluids* (Springer, 1996).
17. I. S. Poperrechny, Combined rotational diffusion of a superparamagnetic particle and its magnetic moment: Solution of the kinetic equation, *J. Mol. Liq.* **299** (2020) 112109.
18. Y. L. Raikher and V. I. Stepanov, Nonlinear dynamic susceptibilities and field-induced birefringence in magnetic particle assemblies, *Adv. Chem. Phys.* **129** (2004) 419–588.
19. Y. L. Raikher and V. I. Stepanov, Physical aspects of magnetic hyperthermia: Low-frequency ac field absorption in a magnetic colloid, *J. Magn. Magn. Mater.* **368** (2014) 421–427.
20. D. B. Reeves and J. B. Weaver, Approaches for Modeling Magnetic Nanoparticle Dynamics, *Crit. Rev. Biomed. Eng.* **42** (2014) 85–93.
21. D. B. Reeves and J. B. Weaver, Combined Néel and Brown rotational Langevin dynamics in magnetic particle imaging, sensing, and therapy, *Appl. Phys. Lett.* **107** (2015) 223106.
22. H. Rogge, M. Erbe, T. M. Buzug and K. Lüdtke-Buzug, Simulation of the magnetization dynamics of diluted ferrofluids in medical applications, *Biomed. Tech./Biomed. Eng.* **58** (2013) 1–9.
23. M. Shliomis and V. Stepanov, Theory of the dynamic susceptibility of magnetic fluids, in *Relaxation Phenomena in Condensed Matter*, Advances in Chemical Physics, Vol. 87, ed. W. Coffey (John Wiley & Sons, 1994), pp. 1–30.
24. M. Shliomis and V. I. Stepanov, Rotational viscosity of magnetic fluids: Contribution of the Brownian and Néel relaxational processes, *J. Magn. Magn. Mater.* **122** (1993) 196–199.
25. S. V. Titov, W. T. Coffey, Y. P. Kalmykov, M. Zarifakis and A. S. Titov, Coupled physical and magnetodynamic rotational diffusion of a single-domain ferromagnetic nanoparticle suspended in a liquid, *Phys. Rev. E* **103** (2021) 052128.
26. I. Torres-Díaz and C. Rinaldi, Recent progress in ferrofluids research: Novel applications of magnetically controllable and tunable fluids, *Soft Matter* **10** (2014) 8584–8602.

27. D. A. Varshalovich, A. N. Moskalev and V. K. Khersonsky, *Quantum Theory of Angular Momentum: Irreducible Tensors, Spherical Harmonics, Vector Coupling Coefficients, 3nj Symbols* (World Scientific, 1988).
28. A. Vázquez-Quesada, T. Franke and M. Ellero, Theory and simulation of the dynamics, deformation, and breakup of a chain of superparamagnetic beads under a rotating magnetic field, *Phys. Fluids* **29** (2017) 032006.
29. J. Weizenecker, The Fokker–Planck equation for coupled Brown–Néel-rotation, *Phys. Med. Biol.* **63** (2018) 035004.
30. H. Ye, Z. Shen and Y. Li, Computational modeling of magnetic particle margination within blood flow through lammps, *Comput. Mech.* **62** (2018) 457–476.